TARGETING LOWER MOTOR NEURONS USING RECOMBINANT ADENO-ASSOCIATED VIRAL VECTORS

By

KEVIN DAVID FOUST

A DISSERTATION PRESENTED TO THE GRADUATE SCHOOL
OF THE UNIVERSITY OF FLORIDA IN PARTIAL FULFILLMENT
OF THE REQUIREMENTS FOR THE DEGREE OF
DOCTOR OF PHILOSOPHY

UNIVERSITY OF FLORIDA

2007

To all who helped me achieve my goals.

ACKNOWLEDGMENTS

Members of the Mandel, Reier and importantly the Flotte laboratories aided in this research in countless ways, both technically and intellectually.

TABLE OF CONTENTS

page

LIST OF FIGURES

Abstract of Dissertation Presented to the Graduate School
of the University of Florida in Partial Fulfillment of the
Requirements for the Degree of Doctor of Philosophy

TARGETING LOWER MOTOR NEURONS USING RECOMBINANT ADENO-ASSOCIATED VIRAL VECTORS

By

Kevin David Foust

May 2007

Chair: Terence Flotte
Major: Medical Sciences--Genetics

Neurodegenerative diseases such as amyotrophic lateral sclerosis (ALS) and spinal muscular atrophy (SMA) are particularly devastating in that they rob patients of physical capabilities while sparing their cognitive ability. Currently there are no treatments available for these diseases. The cells primarily affected in ALS and SMA are the lower motor neurons (LMN) that reside in the ventral grey matter along the entire length of the spinal cord. In animal models of ALS and SMA, gene therapies have shown potential in slowing disease progression. However the transition from treating rodents to humans presents a new set of obstacles. Efficiently delivering the gene therapy to the LMN is the first step in bringing a potential treatment to the clinic. We examined novel delivery routes to administer recombinant adeno-associated virus (rAAV) or its secreted transgene product to the entire spinal cord. The first delivery method entailed intravenous or intraperitoneal rAAV8 GFP injections in neonatal mice which resulted in few instances of LMN transduction. Interestingly, these systemic injections efficiently transduced the dorsal root ganglia. The second delivery method was designed to efficiently deliver secreted trophic factor to all levels of the spinal cord after a single intracerebral injection procedure. rAAV5 GDNF was administered to the red nucleus or primary

motor cortex in the brains of adult rats. At 13 weeks post injection, high levels of GDNF were detected in all levels of the spinal cord using ELISA and immunohistochemistry. This novel anterograde delivery method was applied to ALS rats. Administration of GDNF in the spinal cord of the rats showed no therapeutic benefit in the ALS model. Anterograde delivery may still be useful for models of spinal cord injury or for anatomical tracing studies. Indeed, other transgenes may still hold promise for treating ALS.

CHAPTER 1
INTRODUCTION

Spinal Muscular Atrophy

Spinal Muscular Atrophy (SMA) is a neuromuscular disorder that affects lower motor neurons (LMN). LMN reside in the ventral grey matter along the length of the spinal cord. They send axonal projections out of the spinal cord via the ventral roots. The axons make connections at the motor end plate on muscle fibers. This connection is known as the neuromuscular junction (NMJ). In SMA, the integrity of the connection between the axon and muscle is lost (1). The axons begin dying back, a process that eventually leads to motor neuron cell loss (2). Subsequent to denervation, the muscles atrophy leading to a flaccid paralysis. Eventually, paralysis is seen in the intercostals and diaphragm muscles leading to respiratory weakness. Respiratory failure is the ultimate cause of death in the most severe forms of SMA. SMA is the second most common autosomal recessive genetic disease, second only to Cystic Fibrosis. SMA occurs in approximately 1 out of 6000 births, with a carrier frequency of 1 in 35 (1). The most severe forms of SMA occur in newborns and lead to death within the first 2 years. There are also later onset, less severe forms of SMA that do not result in death.

SMA is caused by deletions or defects in the Survival Motor Neuron 1 (SMN1) gene located on chromosome 5q13.3 (3). This chromosomal region is highly unstable and underwent a duplication event leading to a second, nearly identical gene called SMN2. SMN1 and SMN2 encode the same protein. The significant difference between the two genes is a single C→T transition within exon 7 (4, 5). This base change either produces a splice repressor or deletes a splice enhancer (6, 7). The net effect leads to exclusion of exon 7 in 80-90% of transcripts generated from SMN2. This results in a truncated, less stable version of the SMN protein (8, 9). In the presence of at least a single intact copy of SMN1, which makes predominantly full length

SMN (flSMN) transcript and protein, SMN2 splicing defects cause no problems. However disease arises when both copies of SMN1 are mutated or deleted leaving only SMN2 to produce the full length protein. This results in 10-20% of flSMN protein which is insufficient to prevent the aforementioned degeneration.

To model SMA for further studies, knockout mice were created. Mice are different than humans in that they only have one copy of the Smn gene (10, 11). Mouse Smn is most similar to the human SMN1. Deletion of the mouse Smn gene resulted in early embryonic lethality (12). In order to overcome the embryonic lethality, a number of approaches were taken. Two groups added human genomic SMN2 transgenes onto the null mouse background (13, 14). Addition of human SMN2 rescued the embryonic lethality and gave mice with very severe symptoms including smaller size when compared to normal littermates, limb tremor and a rapid degeneration that resulted in death between 4-6 days after birth.

Both spinal and facial motor neuron counts started similar to wild-type littermates at P1 but decline rapidly at P3-5. These severely affected mice were shown to have 1-2 copies of the SMN2 transgene. Other founder lines generated had as many as 8 copies of the SMN2 transgene and showed no disease phenotype with the exception of a short stubby tail. Otherwise, the 8 copy mice were reported to have a normal life span. This rescue of embryonic lethality and modification of disease severity by SMN2 correlate well with data from the patient population. There has never been a null allele SMA patient, and there is a correlation between delayed age of onset and disease severity with increased SMN2 copy number in humans (15, 16). These two facts suggest a gene replacement strategy may hold therapeutic benefit to these patients.

Cre-lox mediated, tissue specific deletions of exon 7 of the mouse Smn allele have also been generated to circumvent the embryonic lethality of Smn knockout. The neuron restricted

knockout mice show severe motor defects and a greatly reduced life span (~25 days) (17). There are nuclear abnormalities in the LMN and signs of denervation atrophy in the muscle. The same group also generated a muscle-specific excision of Smn exon 7 (18). The muscle excision model expresses cre recombinase under the human α skeletal actin promoter, resulting in cre-mediated gene excision in myofibers. Mice with myofiber specific excision of Smn exon 7 deletion lived 33 days on average, and they display a severe muscular dystrophy but no LMN abnormalities. The same group also showed that excision of Smn exon 7 restricted to liver resulted in embryonic lethality (19). On the surface, these tissue-specific knockouts suggest other tissues have roles in disease pathology. However, these models do not accurately recapitulate disease. In humans, all cells have a basal level of flSMN protein which is required for viability. Unlike humans, the cre-lox system in engineered mice completely depletes individual cells of flSMN. Additionally, the cre recombinase activity across different tissues is variable, resulting in a mosaicism of cells with completely intact flSMN or completely depleted flSMN.

A five day survival leaves too short a time interval for therapeutic intervention in the severe SMA mouse model. The addition of a missense A2G SMN1 mutated cDNA transgene onto the SMN2;$Smn^{-/-}$ background improved mouse survival (~227 days) (20). The A2G mice show physiological signs of denervation by electromyography. Histology demonstrated sprouting of adjacent axons presumably attempting to compensate for the diseased axons. Examination of the muscle revealed signs of denervation, and there was a 30% decrease of LMN in the spinal cord. Finally, the most recent SMA model created, added an SMNΔ7 cDNA on the SMN2;$Smn^{-/-}$ mouse background (2). The truncated isoform of the SMN protein is less stable and degraded rapidly within cells. However, it was also suggested, partially based on the tissue specific knockouts, that SMNΔ7 has a detrimental effect. In fact, quite the opposite is true.

Additional expression of the SMNΔ7 transgene increased survival over the 5 day model. As in other models, SMNΔ7 show signs of denervation atrophy in muscle, decreased innervation using NMJ labeling and reduced numbers of LMN, all hallmarks of SMA pathology. The new mouse models have proven to be very important to the field of SMA research, both from a therapy approach and for helping to understand SMN's role in disease.

A mystery in SMA is the pathological cascade that leads to specific LMN disease. The mystery comes from the nature and function of SMN. SMN is a 294 amino acid protein with no known homology. It is a ubiquitously expressed protein with cellular localization in the cytoplasm and nucleus. Within the nucleus it is found in discrete structures called gems. These gems have been shown to colocalize with Cajal bodies. Cajal bodies are involved in RNA transcription and processing. Investigations into the functions of SMN show that it is involved in the housekeeping function of snRNP biogenesis (21). SMN carries out this function as part of a large complex associated both with itself and a number of other proteins called Gemins. An important function of the SMN complex is the appropriate assembly of Sm proteins for splicing (22). Roles of Gemin 2 and 8 in the SMN complex have recently been elucidated (23, 24). It is unclear how disruption of a ubiquitous function leads to degeneration of strictly LMN. There are two theories as to why SMA is a LMN disease. The first suggests that defects in snRNP biogenesis are responsible for LMN degeneration. The implication is that LMN have a higher energy requirement than most cells and are, therefore, less tolerant to inefficiencies in snRNP biogenesis. In support of this argument, Winkler, et al. knocked down either SMN or Gemin 2 transcript in zebrafish using morpholinos resulting in axonal pathfinding defects (25). Morpholinos are modified antisense RNAs that block translation in a sequence specific, dicer independent manner. To compensate, Winkler co-injected U snRNPs and restored axonal

morphology to that seen in the control morpholino group. Addtionally, restoration of U snRNP rescued axonal morphological defects after injection of Gemin 2 morpholinos. The significance of this finding is that the U snRNP production is dependent on the SMN complex. Morpholinos targeting SMN and, importantly, Gemin 2 led to axonal defects that were corrected with the supplementation of intact U snRNP. The authors hypothesized that it is the snRNP biogenesis that is responsible, directly or indirectly, for the tissue specific phenotype seen in SMA.

An alternative hypothesis for the LMN pathology in SMA is that SMN has an as yet undetermined motor neuron specific function. Besides the nuclear and cytoplasmic localization of SMN protein, it has also been found in axons and growth cones without Gemin 2 (26). It has also been shown that Sm proteins are not found in growth cones (27). SMN has also been shown to undergo bi-directional axonal transport in affiliation with microtubules. SMN can bind β-actin mRNA and is required in conjunction with hnRNP R for its proper transport to the axonal growth cone (28). Two recent papers have investigated axon specific roles for SMN. Setola, et al. isolated a previously unknown SMN transcript and protein from rat spinal cord (29). This protein is truncated and results from the inclusion of intron 3 which contains an in-frame stop codon. This transcript is developmentally regulated and provides for a number of axon specific characteristics. Immunofluorescent staining from rat spinal cord showed axonal and peripheral membrane localization of the new protein termed axonal SMN (a-SMN). Overexpression of a-SMN in a neuronal cell line resulted in altered cell morphology and increased neurite sprouting (29). In addition, when overexpressed in HeLa cells, a-SMN leads to cellular extensions in which a-SMN colocalizes with F-actin, a growth cone marker (29). Axonal-SMN over expression also yields increased axonal lengths when over expressed in a neuronal cell line compared to flSMN. The significance of this finding for disease is unclear. When analyzed in a

human cell line, the transcript that generated a-SMN came from SMN1 based on sequence information. However there is no clear reason why it couldn't be generated from SMN2 also. Therefore, loss of SMN1 shouldn't result in loss of a-SMN (29).

A second study arguing for an axon specific role of SMN regards the zebrafish morpholino model. Carrel, et al. (30) injected zebrafish embryos with morpholinos targeting SMN transcript. In a series of experiments, these investigators supplemented the SMN knock down with different mutant SMN transcripts including SMNΔ7 and SMNΔ7-VDQNQKE. Carrel, et al. found transcripts that could rescue axonal defects caused by SMN knock down yielded proteins that did not complex which is required for snRNP biogenesis. In addition, this study also showed that SMN mutations that did have snRNP assembly activity were unable to rescue the axonal defects in the zebrafish. Interestingly, SMN morpholino mediated knock down led to reduced survival in the zebrafish model. The reduced survival was only partially rescued by expression of transcripts that rescued axonal morphology. The authors speculated that peptide replacement were only transiently expressed and may be required for later functions or axon maintenance. The fact that only the zebrafish model shows axonal pathfinding defects with SMN reduction. Therefore, conclusions about SMN function taken from the zebrafish model are difficult to interpret relative to the human. In humans, there are less severe forms of SMA with juvenile and adult onset indicating developmental and adult axon health.

Amyotrophic Lateral Sclerosis

Amyotrophic Lateral Sclerosis (ALS) is predominantly a late-onset fatal neurodegenerative disorder. ALS is thought to mainly affect α spinal and facial motor neurons, although there is some corticospinal tract involvement in the late stages of disease as well. After initial onset of muscle weakness, patients progress to paralysis and eventual respiratory failure within 3-5 years.

There are two categories of ALS; sporadic and familial. Familial ALS is responsible for 10-20% of reported cases. Of these familial cases, the most studied mutations are in the Cu/Zn SOD1 gene. The genetics of familial ALS are complicated and a complete discussion can be found in Kunst (31).

Most often SOD1 mutations are autosomal dominant. Presently over 100 mutations linked with disease have been identified, and nine have been used as transgenes to generate animal models of ALS. Most transgenes in these animal models are expressed on normal mouse or rat SOD1 backgrounds. Therefore, there is an increased amount of total SOD1 expression. Effects of SOD1 over expression vary depending on the mutant allele present. Interestingly, SOD1 knockout mice develop normally and only display an abnormal phenotype in response to axonal injury (32).

A number of gene therapy approaches, using rAAV or other vector systems, have been attempted on the G93A SOD1 mouse model (33, 34). These commercially available mice contain ~18 copies of a human G93A allele on a B6/SJL background. Reports of disease onset vary from 80 to 100 days. The survival limit, as defined by an animal's inability to right itself when placed on its side within 30 seconds, is anywhere from 120-150 days. The variability between animals in a given SOD1 transgenic animal model has yet to be explained. However variability in disease progression in humans carrying the same SOD1 mutations has also been reported, suggesting the presence of some modifying factor, whether genetic or environmental. In transgenic mice, symptoms begin with hind limb weakness and ataxia then progress to weight loss and eventual paralysis.

The G93A transgene has also been expressed in rats by two groups of investigators (35, 36). In rat models, G93A levels were expressed at 8 fold and 2.5 fold over endogenous wtSOD1

in Sprague-Dawley rats. Onset and survival ages were 115 and 126 days in rats exhibiting 8-fold over expression and 123 and 131 days in animals exhibiting 2.5 fold SOD1 over expression. Both groups reported unilateral hind limb weakness as the initial overt symptom, though Nagai, et al (36). described a reduction in spontaneous movement prior to more obvious symptoms. In both rat models, the disease progressed rapidly with severe weight loss and paralysis at the end stage.

All of these animals faithfully reproduce the hallmark pathology of ALS in humans. For a recent review of ALS pathology the reader is referred to Bruijn, et al (37). A great number of pathological events have been detailed in ALS rodent models. A number of events characterize ALS within the α motor neurons. First, with respect to familial SOD cases of ALS, there is a toxic gain of function introduced by the SOD1 mutations, including G93A. Interestingly, in many SOD1 mutations, normal dismutase activity is still present. Normally, Cu/Zn SOD1 acts as a homodimer. Each subunit binds one zinc and one copper ion. The copper has been shown to be important for normal dismutase activity. Additionally, it has been theorized that some ALS mutations can reduce affinity for Zn and lead to aberrant chemistries (38) such as the production of peroxynitrite or hydroxyl radicals. However, those theories are dependent on the SOD enzyme having appropriate copper atoms in the absence of zinc. It was later shown that a mutant missing all of its copper coordinating residues still causes motor neuron disease (39).

One of the hallmark pathologies of neurodegenerative diseases such as Parkinson's, Huntington's and Alzheimer's diseases is intracellular inclusions (40). ALS animal models have been shown to have intracellular inclusions that are immunoreactive to SOD1 and ubiquitin (37). The role, pathological or otherwise, of these inclusions in ALS has not been determined. Theories to explain the function of these inclusions are an overloaded proteasome, depletion of

protein folding chaperones or sequestration of normal functioning proteins. Intracellular inclusions are found in both sporadic and familial cases of ALS (37). The absence of SOD1 from the protein aggregates in the sporadic cases is noteworthy (41). Lack of SOD1 involvelment in both forms of disease suggests an underlying mechanism independent of SOD1 contributes to the etiology of both forms of disease.

Various lines of evidence suggest that mitochondria play an important role in ALS disease progression. Higgins, et al. (42) described mitochondrial degeneration involving the expansion of the mitochondrial outer membrane leading to an increase of the intermembrane space in G93A mice. Mitochondrial expansion involved recruitment of peroxisomes to the mitochondrial vacuolizations, mutant SOD1 accumulation within the intermembrane space and eventual loss of cytochrome c staining in the mitochondria. It has been hypothesized that the decrease in cytochrome c within the mitochondria could reflect its release and triggering of apoptotic events (37). Indeed, activation of caspase-1, -3 and -9 have all been demonstrated in response to mutant SOD1 (43, 44). Dupuis, et al. (45) demonstrated that G86R SOD1 mutants exhibited a hypermetabolic state in muscle which can be counteracted by feeding the animals a high fat diet, thereby increasing survival by 20%.

In addition to muscle, other non-neuronal cell types are implicated in ALS such as astrocytes and microglia (37). Gliosis accompanies hind limb weakness and motor neuron loss in SOD1 animal models (35). Therefore, defective glutamate clearance by astrocytes maybe an explanation for the increased glutamate levels in the cerebrospinal fluid of ALS patients. Howland, et al. (35) showed decreased immunoreactivity and function of excitatory amino acid transporter 2 (EAAT2) in spinal cords of end stage of the G93A rat. EAAT2 is the predominant

glial glutamate transporter in the CNS, and defective clearance of glutamate from the synapse can lead to excitoxic death of the motor neurons.

Microglia may also play a role in ALS pathology. Microglia are the immune cells of the CNS, and can exist in activated or resting states. In the activated states, microglia mediate a response by secreting cytotoxic and inflammatory molecules. In ALS, there is proliferation and activation of microglia in areas of motor neuron loss. Thus application of minocycline, an antibiotic that can also block microglial activation, slowed disease progression in mutant SOD mouse models of ALS (46, 47).

Even with all that is known about the pathology in ALS animal models, the etiology of ALS remains a mystery. When SOD1 mutations are restricted to either astrocytes or neurons, they are not sufficient to cause ALS in mice (48-50). However, when chimeric mice produced by blastocyst injection or morula aggregation of wild type and mutant SOD containing cells are constructed, the disease course is modified (51). More importantly, low percentages of wild type non-neuronal cells can rescue mutant SOD expressing motor neurons from degeneration. Finally, Clement, et al. demonstrated that mutant SOD1 expressing non-neuronal cells can convey ALS-like pathological properties to normal neighboring motor neurons. The data from chimeric mice suggests that SOD1 mutations do not kill LMN in a cell autonomous fashion.

The significance of these findings is of particular interest to those who wish to treat ALS using gene therapy because they make it difficult to identify the appropriate target cell population; motor neurons, glia, another tissue or some combination. Indeed, targeting motor neurons or glial cells of the spinal cord alone is a tremendous challenge in itself. Although the diseased cell population in SMA is more defined (LMN), the problem of effective delivery of a therapeutic gene product still remains. Our studies used adeno-associated viral vectors (AAV) to

target the spinal cord. After a brief introduction of AAV vectors, delivery routes of viral vectors to the spinal cord will be discussed.

Adeno-Associated Viral Vectors For Gene Therapy

Recombinant adeno-associated virus (rAAV) vectors are unique among the vector classes currently available for human gene therapy in that they are based upon a class of viruses that commonly inhabits a human host without causing any detectable pathology. This fact, combined with the propensity of AAV to establish long-term persistence in non-dividing human cells, lead to the idea that this class of vectors would be ideal for a variety of gene therapy approaches (52).

AAV is member of the genus Dependovirus, of the virus family Parvovidae, subfamily Parvovirinae (53). Although the vast majority of work with AAV reported in the literature up until 5 years ago was with AAV2, over 100 serotypes and genomic variants of AAV have now been reported, and many display transduction and biodistribution characteristics that differ from AAV2 (52). AAV is a single-stranded DNA-containing non-enveloped icosahedral virus that was first discovered as a contaminant of adenovirus cultures, and subsequently was found to be a common inhabitant of the human respiratory and gastrointestinal tract (54). AAV generally require a helper virus, such as adenovirus, herpesviruses, or vaccinia, in order to replicate in the productive phase of its life cycle. In the absence of helper virus, AAV has the capacity to establish long-term latency within mammalian cells (53). AAV possesses several features that are unique among mammalian viruses, including the non-pathogenic nature of AAV infections and the capacity of AAV2 to integrate its proviral DNA into a specific region of human chromosome 19, the AAVS1 site (55).

When cells latently infected with AAV are subsequently infected with a helper virus, the AAV can be rescued and reenter the replicative phase of the life cycle. AAV is capable of carrying out all functions necessary for completing its life cycle with a remarkably small (4.7kb)

and simple genome structure (53). There are two genes, rep and cap, flanked by two inverted terminal repeats (ITRs) which contain all the *cis*-acting sequences necessary for packaging, replication, and integration of the vector genome (53). Recent studies also indicate that the ITRs possess some transcriptional promoter activity, albeit relatively weak (56, 57). The crystal structure of AAV2 has recently been published (58). The structural determinants of AAV2 receptor binding to the heparan sulfate proteoglycan attachment receptor have also been delineated by various mutagenesis studies (59, 60). The differences in binding affinity to different receptors among the various serotypes can be accounted for by differences within these structural determinants. rAAV vectors were originally constructed by deleting portions of the AAV rep and cap genes and replacing these with genes of interest, demonstrating that only the ITRs are required in *cis* for replication and packaging of rAAV genomes, so long as rep, cap, and helper virus functions are provided in *trans* (61). The packaging limit of rAAV is approximately 5 kb.

Refinements of the rAAV packaging and purification process have enabled the use of high titer pure vector (61). Recent protocols have emphasized a potential increase in upstream production yields by using Ad gene plasmids in lieu of active Ad infection of packaging cells, and by moderating the amount of long Rep (Rep78 and Rep68) proteins expressed relative to short Reps (52/40) and capsid (61). Current purification strategies have sought to avoid CsCl ultracentrifugation, which results in less infectious vector, and favoring column chromatography methods (61).

The availability of high-titer, highly purified rAAV2 vector preparations, free of replication-competent (rc)-AAV has allowed for testing of rAAV2 gene delivery in numerous *in vivo* settings, including many rodent and nonhuman primate models (62). rAAV gene delivery

was first demonstrated in the lungs of rabbits, mice, and rhesus macaques in the context of the development of rAAV2-CFTR vectors for the treatment of cystic fibrosis (CF) (62). These studies indicated that rAAV2 gene delivery to the lung was feasible, safe and persistent. Surprisingly, persistence was associated with stable episomal forms of the vector genome, rather than with integration (63). Indeed, the crucial role of the rAAV Rep protein (which is deleted from most rAAV2 vectors) in driving integration has since been confirmed (64, 65). Subsequent studies showed that rAAV2 gene delivery was much more efficient in terminally differentiated neurons, retinal cells, myofibers, and hepatocytes (66).

The use of AAV for gene therapy in animal models of muscular dystrophies, such as the mdx-deficient mouse and models of sarcoglycanopathies, have also recently been published (67-69). rAAV2-based gene delivery to muscle and liver has been shown to be quite effective for delivery of secreted proteins, such as factor IX and alpha-1 antitrypsin (70, 71). Subsequent studies have indicated that mechanisms beyond cell-surface attachment may account for some of the serotype specific differences in gene transfer efficiency (72). Nuclear entry may be a limitation in some contexts, and can be enhanced by inhibition of proteosome function (73).

In any case, the newly widened availability of alternate AAV capsid serotypes and receptor-specific mutants promises to provide means for bypassing the various obstacles to vector entry. For instance, AAV5 appears to bind primarily to N-linked sialic acid, while AAV4 binds to O-linked sialic acid. With the exception of AAV2, co-receptors required for efficient entry have not been identified. In the case of AAV2, it appears that either alphaV-beta5 integrins or the fibroblast growth factor receptor-1 can function as a co-receptor (74, 75).

The use of rAAV2 in early phase clinical trials has been reported for several diseases including cystic fibrosis (CF), hemophilia B, α-1-antitrypsin deficiency and Canavan disease

(76-82). In the case of CF, three phase I trials and two phase II trials have been performed (77, 83). The phase I trials have included delivery to the nose, maxillary sinus, and lung, with the latter organ approached both by direct bronchoscopic instillation and by aerosol inhalation. Phase II studies of maxillary sinus and aerosol administration have also been completed recently. Taken together, these studies generally indicate a lack of any vector-mediated toxicity, and a surprisingly efficient rate of DNA transfer. The phase II aerosol trial also showed evidence of a decrease in pulmonary inflammation and an increase in pulmonary function, both of which were statistically significant in this randomized, placebo-controlled, double-blinded study. The effects lasted only for 30 days, however, and repeated administration did not appear to be capable of sustaining the positive effects. This appears to relate to the development of neutralizing antibodies to AAV2 capsid components.

Gene Therapy Delivery Routes to the Spinal Cord

A number of studies have targeted the spinal cord using viral vectors for animal models of disease other than ALS and SMA. These studies have elucidated 6 prominent injection routes that potentially or have demonstrated spinal cord transduction. Some delivery routes allow for direct LMN transduction which can be useful for gene replacement strategies. Other routes transduce projections to and from the spinal cord suggesting a secreted transgene product would be more effective.

Retrograde Delivery

Recently, the most commonly used delivery route for targeting LMN with viral vectors has been to administer the vector intramuscularly. The efficacy of intramuscular delivery requires viral uptake by the innervating axon terminals of the LMN then retrograde transport of the viral particle to the cell body. The requirement for retrograde transport limits the vector choices. Adenovirus, rabies-G pseudotyped lentivirus and rAAV2 have had the most success.

Adenoviral retrograde delivery

Acsadi, et al.used (84) adenovirus vectors to pre-treat SOD1 ALS mice with GDNF and showed improvements in survival and motor neuron counts. Intramuscular injection of recombinant adenovirus expressing BDNF increased LMN counts in a model of chronic spinal cord compression (85). Previously the same group had demonstrated in both normal and compressed mouse spinal cord the ability of recombinant adenovirus to undergo retrograde transport following an intramuscular injection (86).

Lentiviral retrograde delivery

Experiments with lentivirus have also had success. Using equine infectious anemia virus (EIAV) Mazarakis, et al. (87) showed that pseudotyping of the viral glycoproteins resulted in different CNS transduction patterns. Rabies-G protein allowed retrograde transport of the intramuscularly injected virus as opposed to VSV-G pseudotyped virus which did not. Rabies-G EIAV has been used in gene replacement strategies such as delivering the SMN transgene to a mouse model of SMA (88). This is a particularly challenging model in that mice appear normal at birth, show signs of disease at P5 and, if untreated die at P13. Lenti-SMN treatment improved survival by 5 days over untreated animals and 3 days over LacZ treated controls. There were also improvements in lumbar LMN counts. This is the first attempted gene therapy in the 13 day SMA model. It is encouraging that SMN replacement can improve the prognosis of animals and possibly patients. However, to obtain the therapeutic benefit, P2 mice were bilaterally injected in the hindlimbs, face, diaphragm, intercostals and tongue muscles. These are technically difficult injections requiring large volumes of vector.

Lentivirus has also been utilized to treat P7 SOD1 (G93A) ALS mice (89). In this study delivered small hairpin RNA (shRNA) to reduce the expression of the SOD1 transgene by RNA interference. After showing a 40% knock down of mutant SOD1 protein, treatment delayed

disease onset by 115% over empty vector and mistargeted injected animals. Knock down of mutant SOD1 resulted in a 77% increase in survival. EIAV vectors have also had success using secreted molecules to treat ALS. Again, following the same injection route, in P21 or P90 SOD1 (G93A) mice, Azzouz, et al. used rabies-G EIAV to deliver VEGF to the spinal cord. Vector treatment prior to symptoms delayed disease onset by 28 days and increased lifespan by 38 days (90). More importantly, treatment at disease onset increased survival 19 days on average. In this paper, no steps were taken that show that retrograde transport of virus was required for maximal therapeutic benefit (90).

AAV retrograde delivery

Retrograde transport of recombinant adeno-associated virus (rAAV) has also been used to target the spinal cord (91, 92). Initially there were conflicting reports as to the retrograde transport ability of different AAV serotypes. Burger, et al. saw only anecdotal instances of retrograde transport of rAAV2 GFP following injections into the striatum, hippocampus and spinal cord (93). However, they reported serotypes 1 and 5 more commonly undergo retrograde transport within the CNS. Wang, et al. (94)and Lu, et al. (95) injected rAAV2 LacZ in the gastrocnemius of normal mice. In agreement with Burger, neither paper reported β-galactosidase staining of LMN in the corresponding region of spinal cord. Conversely, Kaspar, et al. (96) performed rAAV2 GFP injections into the hippocampus and striatum similar to Burger, et al. Kaspar readily saw retrograde transport of virus after a larger volume (3μl vs 2μl) but a similar titer ($5x10^{10}$ vs $3.6x10^{10}$ particle) injection.

Subsequently, Kaspar, et al. used intramuscular rAAV2 to deliver IGF1 to ALS mice and to yield the largest delay in onset and increase in survival reported in (G93A) mice to date. IGF1 treatment also increased survival by 22 days when rAAV2 IGF1 treatment was given at disease

onset (91). Kaspar further demonstrated that the therapeutic benefit required retrograde transport of the virus to the spinal cord (91). When a VSV-G pseudotyped lentivirus, that does not undergo retrograde transport (87), carrying the IGF1 transgene was given intramuscularly, significantly smaller increases in survival were seen (91). The same methodology was applied in a later paper by Miller, et al. (97) where hind limb treatment with rAAV2 or VSV-G lentivirus delivering siRNA targeting mtSOD1 in ALS mice required the retrograde transport abilities of rAAV2 to see improvements in hind limb grip strength. Finally, Pirozzi, et al. (92) compared intramuscularly injected rAAV serotypes 1, 2, 5, 7 and 8 for their ability to undergo retrograde transport within the LMN of the spinal cord. Four weeks after injecting rAAV β-gal into the gastrocnemius of normal adult mice, gene expression was analyzed in the injected muscle and spinal cord. The authors found that rAAV2 and 1 transduced LMN after intramuscular injection. Quantification of transduced LMN allowed the authors to conclude that rAAV2 gave almost complete transduction of the LMN pool that innervates the gastrocnemius (92). The authors went on to treat a mouse model of hereditary spastic paraplegia using intramuscular injections of rAAV2 Spg7, and saw improvement in rotarod performance sustained for 10 months post injection (92).

The retrograde transport of virus following an intramuscular injection is a promising and relatively easy delivery route to administer gene therapy to the spinal cord. It seems unlikely, though, that the retrograde delivery of virus could be used to treat the entire spinal cord in a human; it may be useful to selectively rescue crucial LMN such as the phrenic pool that innervates the diaphragm. However there are still drawbacks. Most of the aforementioned experiments used very high volumes of virus (100μl per animal). Some experiments injected 5 separate muscle groups with 3 injection sites per muscle. In humans, multiple injections increase

the risk of injection site immune reactions and would require large amounts of virus. Additionally there is a report of defects in retrograde axonal transport in ALS (98). Also in ALS, there is degeneration of the corticospinal tract. It is unclear if the CST degeneration is in response to a LMN defect, but the retrograde transport dependent delivery route would exclude the UMN from treatment. Finally, with regards to rAAV2, if the preclinical data are correct that rAAV2 is the most efficient serotype for retrograde transport, the problem of neutralizing antibodies against rAAV2 within the human population might prevent successful administration in the clinic (99).

Direct Spinal Cord Injection

With the current technology it is impractical to treat LMN diseases like SMA or ALS with direct spinal cord injections. However for sparing or rescue of a defined subset of LMN, for treatment of spinal cord injury or neuropathic pain, direct spinal cord injections hold merit.

Lentiviral spinal cord injection

Pezet, et al. examined the transduction patterns of two different lentiviruses (HIV and EIAV both pseudotyped with VSV-G) after direct spinal cord injection (100). Both vectors transduced neurons. However the HIV based vector predominantly transduced astrocytes and low levels of microglia. Following 2 x 1.5µl injections of ~1 x 10^8 TU of either vector into the dorsal horn of L5 in rats, transduction was seen from L3 through S1. This included both grey and white matter encompassing all spinal cord lamina of the injected side. Guillot, et al. again used lentiviral vectors to directly inject spinal cords of normal adult mice (101). Two injections of 0.5µl (~3 x 10^5TU per site) LV-LacZ approximately 1.5mm apart rostrally yielded LMN labeled approximately 1mm away from the injection site.

Similar injection parameters were used to deliver LV-GDNF to the spinal cord in normal mice. Immunohistochemical detection of the secreted GDNF was seen ~2.5mm away from the injection site. When the LV-GDNF was administered to the facial nucleus and L4 spinal cord of SOD1 (G93A) mice only the facial nucleus injection showed partial rescue of motor neurons from cell death. Raoul, et al. used VSV-G pseudotyped HIV based vectors to deliver siRNA against mtSOD1 in (G93A) mice (102). The authors injected the virus in L3-L4 of 40 day old mice, and concluded that direct spinal cord delivery of a non-diffusible factor failed to improve survival in ALS mice. Therefore they observed electromyographical changes in the hind limbs. siRNA treatment against mtSOD1 delayed onset of disease by 20 days over mistargeted controls (102).

AAV spinal cord injection

Burger, et al. (93) showed strong neuronal transduction in the spinal grey matter of rAAV serotypes 1, 2 and 5 injected animals. They noted high variability in cell numbers and volume transduced in the type 1 and 5 groups. This variability prevented the averages from being significantly different among the serotypes. However individual animals within the type 1 and 5 groups showed much greater numbers of transduced cells and volume when compared to any animals in the serotype 2 group. Xu, et al. (103) studied rAAV2 targeting of dorsal root ganglia (DRG). Following a 2µl direct injection of rAAV2 GFP in the L4-L5 DRG, ~70% of DRG neurons were GFP+ 3 months post injection. GFP+ fibers were also seen innervating the dorsal and ventral horns. The authors noted no transduced cell bodies in the spinal cord.

Direct spinal cord or ganglion injection has a number of potential applications in spinal cord injury and pain management. However for treating a dispersed cell population like LMN, it is too inefficient. Noteworthy for ALS is the ability of HIV based vectors to transduce both

astrocytes and neurons. There is ample data to suggest that ALS pathology results from contributions of multiple cell types (37). Attempts to preserve a specific motor neuron pool in ALS using direct spinal cord injection could benefit by co-transducing neurons and glia in the diseased cord. Finally, DRG transduction may also be beneficial for targeting LMN. DRG cells are part of a reflex arc in which DRG cells simultaneously send projections to the brain and to LMN. DRG transduction may therefore be useful to deliver a secretory molecule, such as a neurotrophic factor, directly to LMN.

Intrathecal Injection

Intrathecal injection targets the subarachnoid space in between vertebrae of the spinal cord. This injection route requires surgically exposing the spinal column without a laminectomy. In human patients, cannulas can be implanted intrathecally that are attached to external infusion pumps that allow for repeated intrathecal administration of drugs (104). Intrathecal administration of recombinant proteins has shown success in ALS animal models and had partial success in clinical trials (104, 105).

Two groups recently delivered rAAV vectors to animal models using intrathecal injections. Intrathecal injections allow for relatively high volumes to be administered with little spread to non-neuronal tissues (106). Watson, et al. evaluated the brain after intrathecal administration of rAAV2 α-L-iduronidase (IDUA) in the lower thoracic region of the mouse spinal cord. Histological examination 3 months post injection revealed labeled cells scattered throughout the brain, with the highest concentrations being in the olfactory bulb and cerebellum (106). Xu, et al. administered rAAV2 GFP intrathecally in the lumbar spinal cord of mice (103). They found labeled cell bodies in laminae I-IV 3 weeks post injection. Following the 5μl unilateral injection, labeled cells were seen up to 2mm in the rostral-caudal axis with labeled fibers seen 6mm away.

However there were no transduced cells contralateral to the injection side indicating limited lateral spread of the virus (103).

Intrathecal administration confines the virus to the CNS limiting accidental transduction of other tissues. It offers the potential of a large dispersal of vector transduction within the CNS without much specificity.

Intracerebroventricular Injection

The ventricle system is a continuous series of large fluid filled spaces in the brain and spinal cord through which cerebrospinal fluid flows. Intracerbroventricular injection (ICV) targets the lateral ventrical in either hemisphere of the brain. Access to it would require a craniotomy and stereotaxic neurosurgery. ICV administration of recombinant VEGF has been shown to delay onset and increase survival in ALS mice (107).

Passini, et al. (108) administered rAAV1 or rAAV2 to neonate mouse brains and showed very different transduction patterns between the two serotypes with respect to the structures transduced. Another important difference was noted during histological examination for the secreted transgene product, β-glucuronidase. Enzyme spread was far greater throughout the rAAV1 injected brain. Unfortunately the authors did not examine the spinal cord. However one year after bilateral ICV administration of rAAV1 β-glucuronidase to mucopolysaccharidosis type VII mice, there was complete reversal of molecular pathology in the brains. Levites, et al. (109) performed similar neonate injections in an Alzheimer's mouse model. They were able to show a 25-50% decrease Aβ deposits after treatment with an rAAV1 vector encoding antibody Fv fragments against amyloid beta.

ICV delivery of rAAV1 in neonatal mice allows widespread gene expression throughout the brain. Its effects on the spinal cord were not investigated in these studies. ICV may be a

useful delivery method for both secreted and intracellular molecules because of its wide distribution transgene expression. Finally, these injections were conducted in neonate mice where the ventricular brain barrier is not established (Bruni JE). Further studies would need to demonstrate vector distribution after administration in adult animals for use in later onset disorders.

Other Delivery Routes

Fu, et al. examined vector distribution after intravenous or intracisternal injections of self-complementary AAV2 (scAAV2) vectors expressing GFP in mice (110). Fu, et al. also tested the ability of infused mannitol to alter CNS transduction after systemic scAAV2 delivery (110). Mannitol is used to temporarily disrupt the integrity of the blood brain barrier (111). Fu found that prior infusion with a mannitol solution was required for CNS transduction (110). At most they found 500 GFP+ brain cells, neurons and glia, after mannitol followed by scAAV2 GFP intravenous injection. Fu also performed intracisternal injections. They injected scAAV2 GFP into the cisterna magna of adult mice, the subarachnoid space between the cerebellum and medulla. The intracisternal injection also benefited from mannitol pretreatment, resulting in GFP+ cells throughout the brain with most of the transduced cells near the cerebral ventricles (110). The spinal cord showed numerous labeled fibers in the ventral white matter of the cervical spinal cord (110).

More recently, other serotypes of rAAV have shown remarkable ability to almost completely transduce skeletal muscle following intravenous or intraperitoneal injection. Wang, et al. administered rAAV8 GFP intravenously or intraperitoneally to normal neonate mice. They found that 5 months post injection, skeletal and cardiac muscle were almost completely transduced (112). Non-muscle tissues, including brain, showed little or no transduction as assessed by cryosections for native fluorescence (112). In a more recent study (113), the same

group treated a hamster model of muscular dystrophy using intraperitoneal delivery of rAAV8 mediated δ-sarcoglycan. Western blots of brains failed to detect transgene product in rAAV8 δ-sarcoglycan injected animals. Southern blots for rAAV genomes also showed very low copy numbers. These three studies confirm rAAV inability to reliably pass the blood brain barrier without a permeablizing agent. Interestingly, Pacak, et al. (114) did show rAAV8 derived β-galactosidase in the brain following neonate intravenous injection, but it is unclear if endogenous galactosidase activity (115)in the brain was investigated. Protein levels in the brain were the highest of the non-muscle tissues examined, but Pacak, et al. failed to investigate the spinal cord. Despite the inconsistencies in the ability of systemically delivered rAAV to enter the CNS, retrograde transport of virus may provide an alternative entry into the spinal cord that does not exist for the brain. A systemic delivery route for human patients would not eliminate the need for large amounts of virus as with repeated intramuscular injections. The potential to target LMN with a single injection versus possibly hundreds of intramuscular injections is worth investigating.

rAAV Gene Therapy for ALS

There is abundant evidence demonstrating the importance of neurotrophic factors to motor neurons in both a normal and injury context. Recently rAAV was used to deliver GDNF, a very potent motor neuron survival factor, to a G93A mouse model of ALS. Wang, et al. administered mice intramuscular injections of rAAV2 GDNF into muscles of all four limbs at approximately 9 weeks of age (94). A total of $1x10^{11}$ genome copies were injected in a volume of 100µl per mouse. GDNF expression in muscle was confirmed by immunohistochemistry. The rAAV delivered GDNF was taken up and retrogradely transported from the periphery to motor neuron cell bodies by detection of the FLAG-tagged protein. However, when a control injection of

rAAV2 LacZ was delivered to muscle no LacZ staining was observed in the spinal cord (94). The authors concluded there was no retrograde transport of intact rAAV2 particles in motor neurons. Treatment prior to symptoms in G93A mice with rAAV2 GDNF delayed disease onset over control by about 2 weeks, and survival was extended 16 days when compared to controls. GDNF treatment did not alter the progression of disease (the time between onset and endstage) (94).

Kaspar, et al. used a similar approach to also treat G93A mice (91). Kaspar used rAAV2 to deliver transgenes for GDNF or IGF1 to hindlimbs and intercostal muscles. At 60 days of age, prior to disease onset, transgenic mice were injected bilaterally with $1x10^{10}$ particles (15µl per site) of rAAV2 GFP, GDNF or IGF1. GFP injected controls displayed disease symptoms at 91 days while onset was delayed 16 days in the GDNF group and 31 days in the IGF group. Survival also increased with rAAV GDNF (11 days) or IGF1 (37 days) treatment. IGF1 treatment produced a maximal life span of 265 days. When animals were treated at disease onset (90 days) GDNF increased survival 7 days while IGF1 increased survival 22 days. The investigators demonstrated their results were dependent upon retrograde transport of the intact virus. They also showed that retrograde transport was dose dependent and quantified over 400 GFP positive motor neurons in the spinal cords after intramuscular injection (91). This is the first such report of reliable rAAV2 transport from the muscle to the spinal cord. The authors hypothesize that differences in vector dose or purification techniques could explain the inconsistency in retrograde transport reports of rAAV2. Regardless, there is a clear difference in the ability of GDNF and IGF1 to increase survival of G93A mice when administered at disease onset. The mechanism of IGF1 action could extend beyond the motor neurons and muscle to include the surrounding astrocytes in the spinal cord.

An increase in astrocyte IGF1 receptor immunoreactivity in ventral horns of G93A mice was recently reported (116). Together with Kaspar's data (91), this suggests that the effect of IGF1 produced in motor neurons likely stretches to surrounding astrocytes as well. The authors state a clinical trial using rAAV2 IGF1 to treat ALS is being planned. Subsequently, Kaspar, et al. demonstrated that the positive effects of rAAV2 IGF1 delivered at disease onset can be improved upon with the addition of exercise (117). G93A mice given running wheels ad libitum at day 40 then treated with rAAV2 IGF1 at Day 90 as previously described showed an 83 day increase in survival. Interestingly, mice exposed to exercise and IGF1 starting at day 90 showed a 37 day increase in survival (117).

To address the dominant nature of the SOD1 mutations in ALS, Miller, et al. (97) used a rAAV2 injection in the right lower hind limb to deliver siRNA against human SOD1 in G93A transgenic mice at 45 days of age. Retrograde transport of the virus to the spinal cord was demonstrated by inclusion of a GFP transgene in the siRNA cassette (97). Treatment with the rAAV2 siRNA targeting SOD1 increased grip strength in the injected hind limb through disease onset. However, grip strength measurements returned to control levels closer to 110 days. Miller, et al. suggested this was due to the upper uninjected part of the limb succumbing to disease. The possible clinical applications of an siRNA directed against SOD1 mutations may be limited due to SOD1 mutations being responsible for approximately 2% of total ALS cases (31). However, if more dominant mutations are linked to ALS, this delivery method could be promising.

Recombinant AAV Gene Therapy For Other Spinal Cord Disorders

Direct intraspinal injection is another route used to deliver rAAV vectors to the spinal cord. Burger et al. also examined intraspinal injection with serotypes 1, 2 and 5. Although there was variation between animals in cell number and volume transduced indicating higher

efficiencies for serotypes 1 and 5 compared with 2, there was no statistically significant difference between the averages among the serotypes tested. Recently, other groups have applied intraspinal injections of rAAV2 for treatment of spinal cord injury and neuropathic pain.

Blits, et al. performed a complete transection and removal of a 3mm segment of rat spinal cord followed by implantation of a Schwann cell bridge (118). Five mm caudal to the graft, the investigators made an injection of rAAV2 BDNF and NT-3 vector cocktail. Significant improvement involving movement of all three limb joints (as measured by the BBB scale) was seen in the neurotrophin groups over the course of the study (118). Prior to the end of the study an anterograde tracer was injected in the spinal cord rostral to the graft. Simultaneously retrograde tracer was injected 6mm caudal to the caudal graft-cord interface. Examination of the retrograde tracer showed a significant increase in labeled neurons in the rAAV2 neurotrophin group compared to control indicating that an increased number of neurons sent projections towards the injection site and graft. Examination of the anterograde tracer showed axons from the intact spinal cord sent projections into the Schwann cell bridge. However no axons exited the graft to enter the caudal spinal cord. The authors suggested their rAAV2 injection was too far from the graft site to promote axonal emergence since the closest transduced cells were still 2mm from the graft-cord junction (118).

The same group has also applied rAAV2 to a ventral root avulsion and reimplantation model. Blits, et al. 2004 avulsed ventral roots from L2-L6 and followed by a lateral reinsertion of root L4 (119). Concomitant to the avulsion and reinsertion, rAAV2 GDNF, BDNF or GFP vectors were injected at the levels of L3 and L5 directed towards the site of injury. Upon histological examination at 1 and 4 months post injection, motor neurons were counted using non-stereological methods. There was a significant improvement in the motor neuron counts

(expressed as % of intact side) in the GDNF and BDNF treated animals compared with control. However, there was no significant increase in choline acetyl transferase (Ch-AT) positive axons in the tibial branch of the sciatic nerve at all time points examined indicating a lack of axonal regrowth by the preserved motor neurons. The authors suggested a more proximal examination of the sciatic nerve could show signs of regrowth. The authors did note an increased number of Ch-AT positive neurites in the ventral horns of rAAV2 GDNF or BDNF treated rats. Blits demonstrated increased sprouting in the trophic factor treated animals but suggested the sprouts did not progress towards the reimplanted root to correctly repair the injury. The authors suggested moving the site of rAAV2 delivery to closer to the reimplantation site would require a delay in vector administration. The authors also propose a removal of the trophic factor to allow for proper pathfinding (119). This could be accomplished with transcriptionally regulated vectors.

rAAV vectors have also been used in pain research. Eaton, et al. used a unilateral chronic constrictive injury (CCI) to the sciatic nerve to test efficacy of rAAV2 BDNF delivery to modulate transmission of neuropathic pain (120). One week after CCI, rAAV2 BDNF or control was injected in the lumbar dorsal gray matter ipsilateral to the nerve injury. Behavioral tests monitoring thermal or tactile hyperalgesia and tactile allodynia were repeatedly administered for 7 weeks post injection. All three tests showed a significant improvement in the BDNF treated animals. The authors note that subsequent research should address the BDNF expression levels required for treating neuropathic pain, as well as any side effects derived from constituitive expression of BDNF in a normal context (120). This again highlights the need for regulatable expression for use with rAAV vectors particularly for neurotrophic factors.

None of the injection routes discussed are ideal candidates for spinal cord targeting. Our work examined other systemic or intracerebral delivery routes of rAAV vectors to efficiently target the spinal cord with either intracellular or secreted transgene products. Our systemic injections sought to minimize discomfort during vector administration as well as reduce the risk of injection site inflammation while simultaneously treating the entire spinal cord. Likewise, intracerebral injections efficiently delivered secreted rAAV5 mediated GDNF to the entire spinal cord in one injection procedure that required smaller amounts of virus compared to intramuscular injections.

CHAPTER 2
MATERIALS AND METHODS

Rat Stereotaxic Injection

200-250g Female Sprague-Dawley rats (Harlan) were anesthetized using isoflurane (1-3%). The tops of their heads were shaved, and the animals were placed into a Kopf stereotax. A tube attached to the nose bar maintained isoflurane anesthesia for the duration of the surgery. Once in place, the skin was cleaned with iodine, then, 70% ethanol. A single anterior-posterior incision was started behind the eyes and extended to the top of the skull. The skin was retracted and held open using Backhaus forceps. The skull was scrubbed clean using sterile cotton swabs and gauzed. 3% hydrogen peroxide solution was used to dry the skull. A 10µl Hamilton syringe (model #80000) was attached to the arm of the stereotax. A pulled Pasteur pipette was attached to the Hamilton needle. AAV vector was drawn up into the syringe; then coordinates for Bregma were taken. The stereotax was subsequently adjusted to the proper anterior-posterior and lateral injection coordinates. The skull was drilled using a rotary drill bit using care not to penetrate the brain. When the skull was paper thin, watchmaker forceps were used to dissect away the skull fragments and reveal dura. Dura was punctured with a 25g needle and dorsal-ventral coordinates were taken. The needle was lowered to the appropriate depth and the injection started. The plunger on the Hamilton syringe was depressed using two air-tight water filled syringes joined by a hose. One end of the water-filled syringe hose was mounted in a microinfusion pump. The other water filled syringe was mounted on the stereotax injection arm above the Hamilton syringe. It was mounted in a manner that as one plunger of the water filled syringe hose was depressed the other plunger was pushed back thereby depressing the plunger on the Hamilton syringe. After completion of the injection, the needle was left in place for 5 minutes to allow for the vector to diffuse away from the injection site. The needle was

withdrawn from the rat head and cleaned using hydrogen peroxide then saline. The incision was closed using wound clips, and the rat was removed from the stereotax.

Neonatal Mouse Injections

The mother (singly housed) of each litter to be injected was removed from the cage. Vector aliquots were placed on Parafilm and subsequently drawn into 0.3cc insulin syringes with 31g needles. The postnatal day 1 (P1) pups were submerged in an ice water bath for 10-20 seconds for anesthetization. For intraperitoneal injections, they were positioned ventral side up and given an injection into the peritoneal cavity of 25µl of $5.3x10^{10}$ AAV particles. Care was taken to avoid any visible milk spot. For intravenous injections, a light microscope was used to visualize the temporal vein (located just anterior to the ear). The needle was inserted into the vein and the plunger was manually depressed. Injection volumes and titers were identical to the intraperitoneal injected animals. A correct injection was verified by noting blanching of the vein. After the injection pups were returned to their cage. When the entire litter was injected, the pups were rubbed with bedding to prevent rejection from the mother. The mother was then reintroduced to the cage.

GDNF ELISA

Rats were anesthetized with an intraperitoneal injection of 0.3-0.5ml of sodium pentobarbital. When the rats did not withdraw from a paw pinch they were decapitated using a guillotine. The brain was removed from the head. Depending on the intended analysis, the brain was bisected into lateral hemispheres, placed in 2ml microfuge tubes, and flash frozen in liquid nitrogen (ELISA); or post-fixed in 4% paraformaldehyde for 48 hours (immunohistochemistry). Spinal cords were carefully removed from the carcass. Once removed, the cord was transversely cut into 6mm long sections. The sections were weighed in 2ml microfuge tubes then flash frozen in liquid nitrogen. The tubes were then stored at -80^{o}C until homogenization. Samples were

analyzed using the Promega GDNF Emax kit. Tissues were homogenized in the buffer described in the kit protocol using a Tissue-Tearor roto/stator type homogenizer. 6mm spinal cord blocks were homogenized in 200µl of lysis buffer, while brain hemispheres received 500µl of buffer. Samples were assayed at 1:5 or 1:10 dilutions and were read using a VersaMax Micro Plate Reader (Molecular Devices). Plate values were adjusted for tissue block weight.

Gait Analysis

A clear plexiglass corridor (90-cm-long, 10-cm-wide runway with 10-cm-high walls) was constructed. At one end of the corridor was a dark goal box. The corridor floor was covered with cash register receipt tape. The room was darkened and spot lights were shone into the clear corridor. The rat's front and hind paws were coated with different colors of non-toxic paint then the rat was immediately placed at the end of the corridor opposite from the goal box. Rats were allowed to run directly to the goal box. Upon entering the goal box, a door was lowered preventing the rat from reentering the corridor. Runs were accepted when the rat proceeded directly to the goal box without stopping in the corridor. Footprints on the receipt tape were measured for stride length and width. Two measurements for stride length and width were averaged per run.

Histological processing

The rats were lethally injected with sodium pentobarbital and transcardially perfused with sterile 0.9% saline followed by 350 ml of 4% paraformaldehyde in 0.01M PBS buffer. The brains were then rapidly removed and post-fixed for 3-12 hrs in the paraformaldehyde solution. The brains were then washed and transferred to a 30% sucrose in 0.01M PBS solution for cryoprotection. Brains were mounted onto a sliding microtome with OCT compound and frozen with dry ice. 40µm sections were divided in 5 series for histological analysis. Tissues for

immediate processing were placed in 0.01M PBS in vials. Those for storage were placed in anti-freeze solution and transferred to -20^{o}C.

Spinal cords were removed from carcasses 24 hours after perfusion then stored at 4^{o}C. Spinal cords were removed using Rongeur forceps to remove the vertebrae. Nerve roots were cut with a scalpel to free the cord from the body. The dura was removed using watch-maker forceps, and then the cord was sectioned into 5-6mm blocks via transverse slice. The caudal surface was marked with a Sharpie, and the block was stored in 1.5ml microfuge tubes filled with 4% PFA. The tubes were stored at 4^{o}C until cutting. Sectioning was performed on a vibratome. 40μm thick transverse sections were cut and transferred in sequence to 96 well plates that were filled with 4% PFA.

Immunohistochemistry

Brain tissue from rats were sectioned, then washed with 0.01 M PBS, then incubated for 15 minutes after the addition of 0.5% H_2O_2 + 10% methanol in 0.01 M PBS. Tissue was again washed and was pre-blocked with 0.01M PBS + 0.1% Triton X-100 and normal serum from the species that the secondary antibody was raised against. Primary antibody solution was added that contained 3% normal serum + 0.1% Triton X-100 in 0.01 M PBS and was incubated overnight at room temperature. Tissue was then washed and a secondary antibody solution added, which contained an appropriate antibody against the species in which the primary antibody was raised, in 3% normal serum + 0.1% Triton X-100 in 0.01 M PBS. The seras were incubated 2 hours and washed again. The color reaction used the ABC Kit (Vectastain Elite, Cat # PK-6100). 1 ml of 2.5 mg/ml 3,3' diaminobenzidine in 0.01 M PBS solution was added and mixed with a final addition of 15 ul of 3% H2O2 in 0.01 M PBS. Tissue was mounted on subbed slides, dehydrated and coverslipped.

Adult rat spinal cord histology was similar to brain histology. The sections were stained as floating sections in 48 well dishes with one section per well. Wells were aspirated to make changes to solutions. Blocking solutions had twice the percentage of serum as the brain protocols and were carried out overnight at room temperature. Primary antibody incubation was also overnight at room temperature.

For neonate mouse spinal cord, paraffin sections (4μm) were de-waxed in xylene and rehydrated through graded alcohol to water. Endogenous peroxidase activity was quenched by incubating sections in 3% H_2O_2 for 10 min. Antigens in spinal cord sections were retrieved by heating in High pH Target Retrieval solution (Dako Cytomation, Carpinteria, CA) for 20 min at 95^{o} C and then cooling for 20 min. Antigens in heart, liver, and muscle sections did not require any retrieval. Nonspecific binding was blocked with Background Sniper (Biocare Medical, Concord, CA) for 15 min. Sections were then incubated with anti-GFP (1:800, Abcam, Cambridge, MA) for 1 h. Signal was visualized by incubating sections in an HRP-conjugated polymer (Biocare Medical) for 30 min. Sections were developed with 3,3' -diaminobenzidine substrate (Biocare Medical), counterstained with hematoxylin (Vector Labs, Burlingame, CA), dehydrated through alcohol series and xylene, and mounted.

Viral Vector Production

All viral vectors were manufactured by the University of Florida Vector Core. The helper plasmid pXYZ5 encodes AAV and Ad gene necessary for creating the pseudotype (i.e the capsid gene from AAV5) (121). The recombinant virus was produced in human kidney epithelial 293 cells from ATCC. These cells were cultured in Dulbecco's modified Eagle medium (DMEM) supplemented with 10% fetal bovine serum and a 1% penicillin/streptomycin antibiotic mixture. Cells were split into a Nunc cell factory 24 hours before transfection so that the confluency at the

day of transfection is between 70-80% or around $1.0x10^9$ cells. Transfections were performed using the conventional calcium phosphate method. Transfection was done by using 1.8mg of helper plasmid pXYZ5 mixed with 0.6mg of the rAAV vector plasmid of interest in a volume of 50ml of 0.25M $CaCl_2$ followed by 50 ml of HBS, pH 7.05, to the DNA/$CaCl_2$. This mixture was incubated at room temperature for 2 minutes at which point the precipitation was halted by the addition of a 1100ml of prewarmed DMEM. These 1100ml of media with the precipitate were then used to replace the media in the cell factory and the 293 cells were allowed to bathe in the calcium phosphate containing media for 60 hours at 37°C and 5% CO_2. The incubation was stopped by removing the media and rinsing the cell with PBS. The cells were dislodged from the cell factory by using 5nM EDTA. The cells were then pelleted by centrifugation at 100g for 10 minutes. The cell were then lysed using 60ml of a solution of (150mM NaCl, 50mM Tris-HCl, pH 8.4), this was followed by 3 freeze thaw cycles using a dry ice ethanol mixture and 37°C water baths. To remove any nucleic acids from the cell lysates they were incubated with Benzonase (Sigma, St. Louis, MO) for 30 minutes at 37°C.

Centrifugation at 4000g for 20 minutes, and the supernatant was then loaded onto a discontinuous Iodixanol gradient. The tubes were sealed and then centrifuged on a Type 70 Ti rotor at 69,000rpm which was equivalent to (350,000g). The virus particles settled at the 60-40% interface of Iodixinol. 5ml of this interface were collected by puncturing the side of the tube with an 18guage needle and syringe. In order to purify and concentrate AAV5 pseudotyped vectors, an equilibrated 5 ml HiTrap Q column (Pharmacia) was used. The column was equilibrated in buffer A containing (20mM Tris-HCl, 15mM NaCl, pH 8.5). The iodixanol fraction containing the vector was diluted with buffer A in a 1:1 ratio and was then passed through the column at a flow rate of 3-5ml/min. Ten volumes of buffer A were used to wash the

column after the iodixanol fraction had been loaded. A second buffer B consisting of (20mM Tris-HCl, 500mM NaCl, pH 8.5) was then used to elute the virus. The virus was then desalted and concentrated using Biomax concentrator with a MW cutoff of 100kD (Millipore, Bedford, MA), the virus was concentrated into PBS or lactated ringers solution. Samples from the vector stock were then run on a 10% SDS–polyacrylamide gel and analyzed with a silver stain to check for protein purity. To quantify the virus, a dot blot assay was performed on the concentrated viral stocks. The dot blot assay was an indirect way of measuring the titer of rAAV virions by detecting the DNA they package. In order to detect only packaged DNA, the sample was first digested for 1 hour at 37^{o}C with a solution of DnaseI (Roche); in 10mM Tris-HCl at pH 7.5 and 1mM Mg Cl_2. This digested any of the unpackaged DNA prior to lysing the virion and releasing the packaged DNA. To release the encapsulated DNA, a solution of 2x proteinase K buffer (20mM Tris–Cl, pH 8.0, 20mM EDTA, pH 8.0, 1% SDS) was used to incubate the sample for 1 hour at 37^{o}C. This degraded the protein capsid and released the single stranded genomes within the virions. The DNA is then precipitated with a phenol and ethanol extraction using glycogen as a carrier. The DNA was then loaded onto a slot blot and immobilized onto a nylon membrane along with a plasmid standard curve .The nylon membrane was then probed for the transgene or the promoter and exposed on film. The signal of the sample is then calculated and compared to the standards and was then back-calculated to a titer. This titer represented DNAse resistant particles.

Genomic DNA Extraction

Genomic DNA (gDNA) was extracted from frozen tissues using the Qiagen DNeasy Tissue Kit. When possible, control tissues were always extracted separately from vector treated tissues. After the extraction procedure, samples were quantified by spectrophotometric analysis to determine the amount needed for real-time PCR.

Real-time PCR

Total copies of the rAAV genome in the mouse tissues were quantified by real-time PCR using an ABI Prism 7700 SDS Sequence Detection System and were analyzed using the SDS 2.0 software. Samples were heated at 50^{o}C for 2 minutes and at 95 degrees C for 10 minutes followed by 45 cycles of 95 degrees C for 15 seconds and 60 degrees C for 1 minute. 0.5ug DNA was assayed for each tissue type. Samples resulting in a copy number greater than 100 copies were concluded to be positive.

CHAPTER 3
SYSTEMIC DELIVERY OF RECOMBINANT AAV8 VECTOR

Experimental Rationale

SMN gene replacement may potentially benefit SMA patients (88). Systemically delivered rAAV8 efficiently transduces skeletal muscle in neonate mice (112, 114). Intramuscular injection of rAAV2 undergoes retrograde transport to the spinal cord (91). Retrograde transport to the spinal cord after systemic injection has not been investigated. Together these technological findings of systemic injections and retrograde transport, suggests an attractive avenue to directly transduce lower motor neurons using rAAV gene therapy in neonate SMA patients. We sought to test the ability of rAAV8 GFP to infect lower motor neurons in normal neonate mice after an intravenous or intraperitoneal injection.

Results

Dams were time mated and monitored daily from embryonic day 17-21. Within one day after birth all pups in the litters were injected with $5.3x10^{10}$ particles of rAAV8 containing the ubiquitously expressed Chicken β−actin hybrid promoter (CB) driving GFP expression in 25µl. Injected pups were sacrificed 5 and 14 days post injection. Front and hind limb skeletal muscle, heart, liver and spinal cord were sampled for analysis. Samples were analyzed via immunohistochemistry for GFP expression and real-time PCR for rAAV genomes.

GFP Immnunohistochemistry

GFP expression was confirmed in heart, liver and skeletal muscle 5 and 14 days after either IP or IV delivery (Figure 3-1). There was no obvious difference in GFP expression between IP and IV injection. However, GFP expression in the liver decreased 14 days post injection.

Examination of the spinal cords from IV injected animals 5 days post injection revealed scattered infrequent GFP expression in ventral horn cells (Figure 3-2). However the dorsal horns and columns were positive for GFP expression. Labeled fibers could be seen innervating the spinal grey matter from the dorsal horns. Spinal cords from IV and IP injected animals 14 days post injection showed similar results to the IV day 5 group (Figure 3-3 through 3-5). There were very few GFP+ ventral horn cells across IV and IP groups. However, the dorsal white matter was completely stained with GFP+ fibers. The fibers travelled laterally across the section to innervate the grey matter (Figure 3-5). Additionally fibers were also ascending in the dorsal columns. Closer examination of the ventral horns showed GFP+ fibers in close proximity to large neuronal cells in the ventral horn (Figure 3-3 B and 3-4 B) and, bouton-like structures were seen to overlap with neuronal cells. No steps were taken to confirm these ventral horn cells were lower motor neurons.

Real-Time PCR Results

Real-Time PCR results showed that heart and liver had the highest vector copy number at 5 days post injection. Skeletal muscles and spinal cords were 1-1.5 logs lower than heart and liver, but had similar copy numbers to each other (Figure 3-6). Liver, heart, tricep and spinal cord all had significant decreases in vector copy number over time ($p \leq 0.05$). When analyzed across injection route, IP injection yielded significantly higher amounts of vector genomes in the tricep compared to IV injection ($p=0.023$). No other tissues examined were significantly different across injection routes.

Discussion

From an AAV gene therapy standpoint, the spinal cord is a fairly inaccessible tissue. This is especially true in the context of lower motor neuron (LMN) diseases. Devising safe and efficient vector delivery methods will be crucial for generating gene therapy treatments for

patients with LMN disease. In this study we compared two different systemic rAAV8 injection routes, intraperitoneal and intravenous, for their ability to directly transduce LMN. After these neonatal injections, we found robust gene expression in heart, liver and muscle in agreement with previous reports (112, 114). However these previous studies failed to examine spinal cord for transduction (112, 114). In this study, GFP protein and rAAV8 genomes reached the spinal cord after a rAAV8 GFP IP or IV injection. Although we did find GFP+ ventral horn cells, their occurrence was irregular throughout the sections examined. On the surface, this suggests retrograde transport of rAAV8 is an uncommon event. Importantly, Kaspar used rAAV2 in their studies demonstrating retrograde transport after intramuscular injection in mice, whereas this study used rAAV8. It has been shown that AAV serotypes use different cell receptors for attachment and entry (52). Once internalized, AAV serotypes are processed differently leading to temporal expression and capsid protein processing differences. It is possible that these differences account for varying efficiencies in retrograde transport of virus.

Another possibility includes the age of animals at vector administration. This study targeted P1 mice while the Kaspar study injected adult mice. The importance of age pertains to the natural elimination process of LMN in the early postnatal period in rodents. A number of studies in neonatal mice and rats suggest 35-75% of motor neurons die between birth and adulthood as part of a normal process with many dying in the first three postnatal weeks (122-125). Therefore it is possible that many of the LMN infected on P1 administration were subsequently eliminated after failing to establish strong synapses at the neuromuscular junction (NMJ). Assuming viral uptake by myelinated motor axons occurs at the exposed axon terminal (i.e. at the NMJ); axons that are shrinking back from motor endplates may be more exposed to circulating virus than those axons engaged in synapse formation. These results suggest that

neither IP nor IV delivery is an optimal injection route using rAAV8 for infecting LMN in neonate mice.

IP and IV rAAV8 injection did yield GFP+ fibers in the dorsal columns, white matter and fibers innervating grey matter. Together, this staining pattern indicates direct transduction of the dorsal root ganglia (DRG). The DRG is a group of psuedounipolar sensory neurons that make up the dorsal root. It is important to note that these cells reside outside the protection of the blood brain barrier (BBB) (126). This means the DRG is exposed to circulating molecules in the blood which would include rAAV virions. Although the GFP staining pattern strongly suggests DRG transduction, the DRG was not preserved during spinal cord dissection. Therefore confirming the observation of DRG transduction is impossible.

DRG transduction could be a useful finding for the treatment of LMN disease. Although this experiment was designed to deliver a gene for an intracellular protein (GFP and eventually SMN) substitution of a secreted molecule, like a neurotrophic factor, could be an important use for DRG transduction. In addition to sending sensory information to the brain via the dorsal columns, the DRG sends projections to LMN or interneurons as part of a reflex arc (126). Synapses on LMN could be an efficient means to deliver neurotrophic factors to diseased cells. Interestingly, synapes on interneurons might also be useful. Transcytosis of neurotrophic factors has been shown to occur in the nervous system (127).

Shifting focus away from LMN disease, DRG transduction could have potential benefit in models of chronic pain. Xu, et al. used rAAV2 DRG or sciatic nerve injection to assess DRG transduction for an animal model of chronic pain (103). Xu observed viral transgene expression in the DRG following direct DRG or sciatic nerve injection. However both injections are invasive procedures. The simplicity of an IP or IV injection could be superior in a human

patient. Despite the ease of systemic delivery, the widespread transduction of other organs such as heart and liver emphasizes the need for tissue specific promoters driving transgene expression to avoid unwanted side effects.

Finally, this study illustrates the pitfalls of gene therapy in the nervous system. Neuronal interconnectivity almost guarantees unintended consequences when targeting a structure in the CNS. While looking for direct LMN transduction, we inadvertently transduced DRG. The DRG also sends direct projections to the thalamus which would in turn receive a secreted gene product. Sustained over expression of trophic factors, such as GDNF, can lead to side effects like aberrant sprouting (128). While these side effects may pale in comparison to the primary disease course, they are still an important consideration when targeting a structure in the nervous system using gene therapy.

In summation, systemic delivery to neonate animals using rAAV8 is not an efficient delivery method to directly infect LMN. For disease models like SMA, alternative means for gene replacement require further investigation.

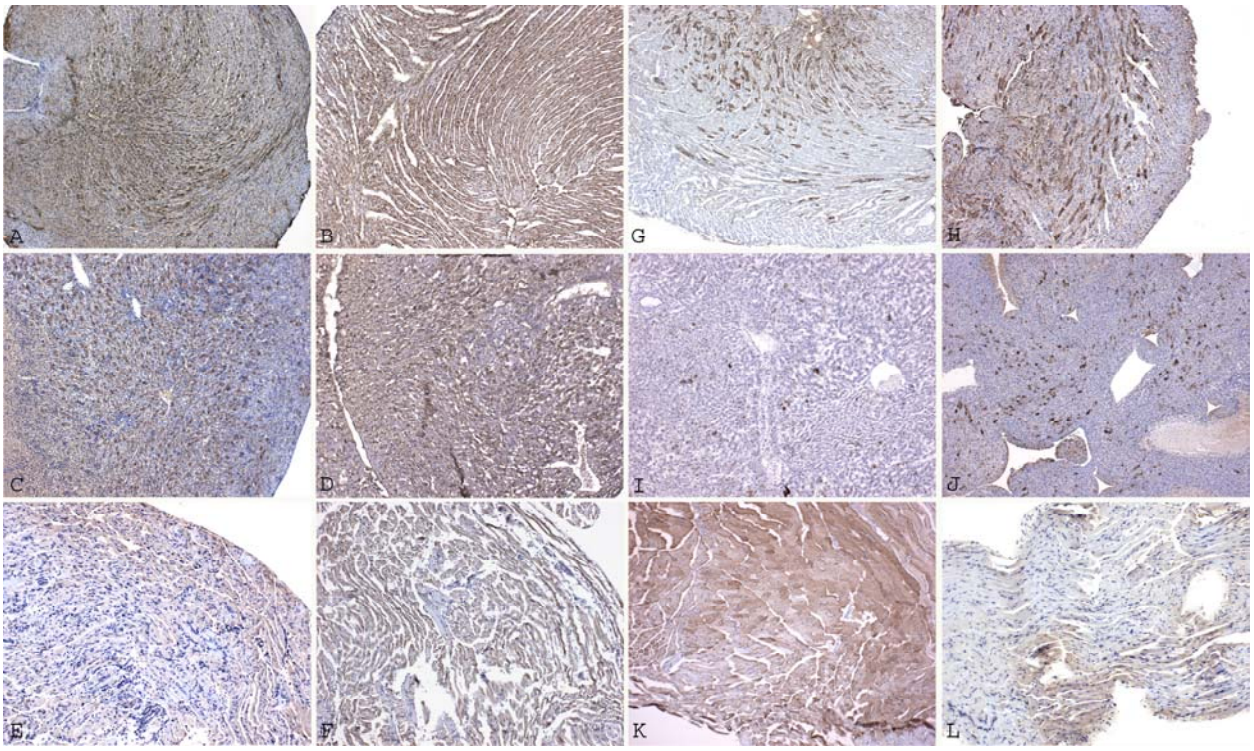

Figure 3-1 Immunohistochemical results for GFP staining in heart (A, B, G and H), liver (C, D, I and J), and skeletal muscle (E, F, K and L). Brown indicates positive staining; blue is a hematoxylin counter stain. The first and second columns from the left are IP and IV day 5 groups respectively. The right columns are IP and IV day 14. With the exception of IP muscle, tissues examined showed a general decrease in positive staining at the day 14 time point.

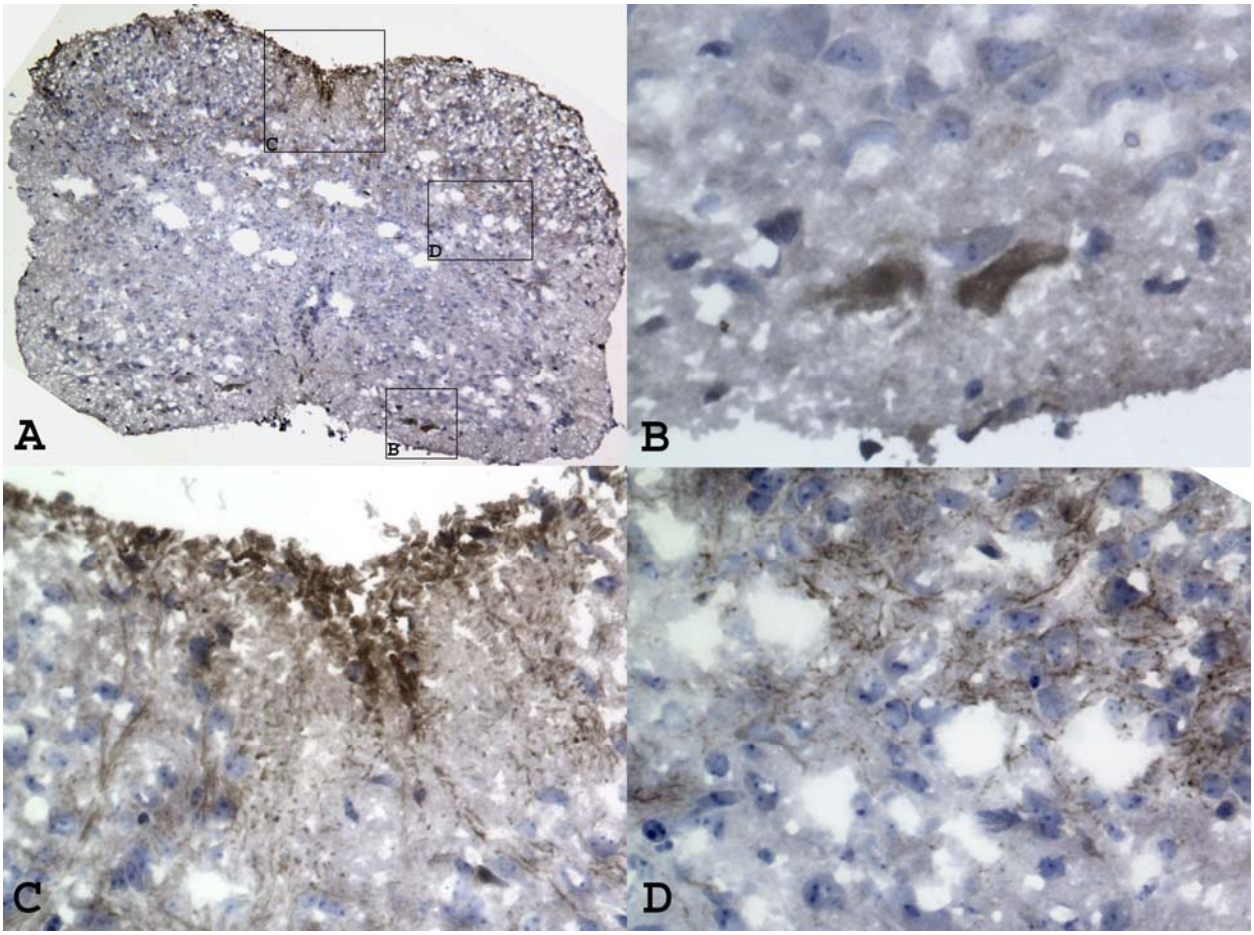

Figure 3-2 GFP immunohistochemistry in the spinal cord harvested from a P5 mouse pup that was injected on P1 intravenously with rAAV8 GFP. (A) shows labeling (brown) in the dorsal white matter and dorsal horns. (B) shows two ventral horn cells expressing GFP. (C) and (D) are taken in the dorsal horns showing labeling of DRG fibers ascending to the brain and innervating the spinal cord grey matter.

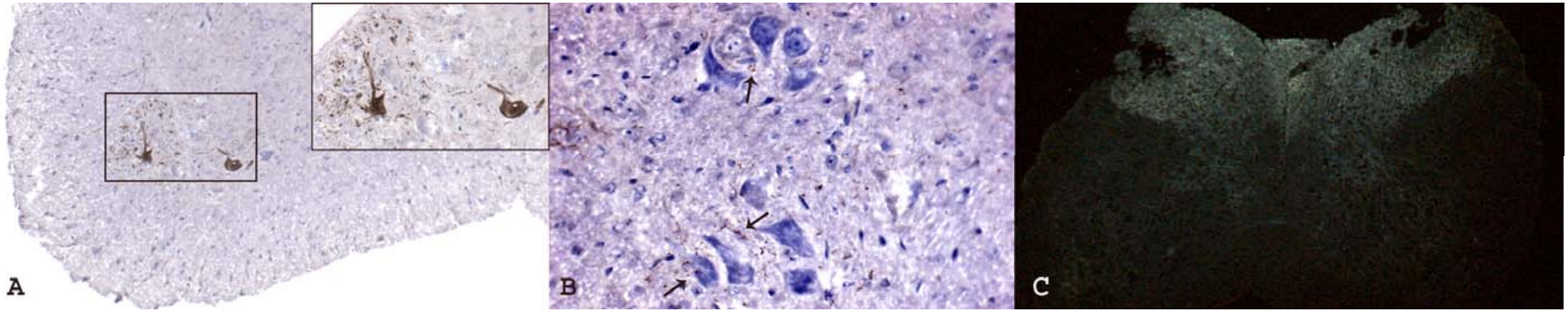

Figure 3-3 GFP immunohistochemical staining of IP day 14 spinal cord. Brown is positive staining; blue is a hematoxylin counter stain. (A) shows two transduced neurons in the ventral grey matter of a sacral section of the spinal cord. The inset shows positive staining in the surrounding grey matter. This is likely dendritic arborization of the labelled cell. (B) shows unlabeled neurons in the ventral grey matter. The arrows point to GFP+ fibers in proximity and overlapping the unlabelled cell bodies. Some labelled fibers show a characteristic swelling indicating a synaptic bouton. (C) is a dark field image of a spinal cord. The gold labelling is the DAB chromagen indicating positive staining. The dorsal horns and white matter show extensive GFP+ fibers. These fibers likely originate from the dorsal root ganglion (DRG), and can also be seen innervating the ventral grey matter.

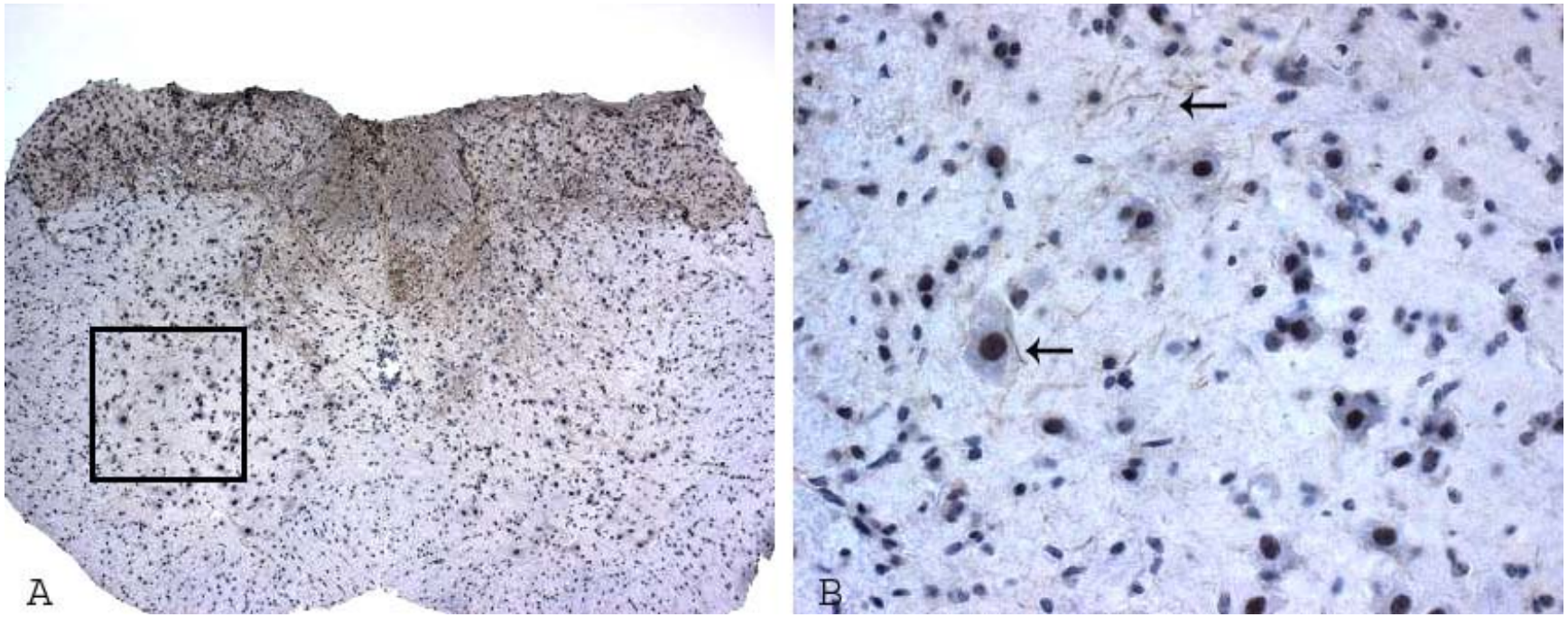

Figure 3-4 GFP immunohistochemical staining of ventral horns of IV day 14 spinal cord. Brown is GFP+ staining; blue is a hematoxylin counter stain. (A) is a low power image of spinal cord. There is a lack of GFP+ cells in the ventral horn. Most of the positive staining is restricted to the dorsal horns and columns. This pattern is indicative of dorsal root ganglion (DRG) transduction. The box indicates the area depicted in (B). (B) shows unlabelled ventral grey matter neurons in proximity to GFP+ fibers (arrows).

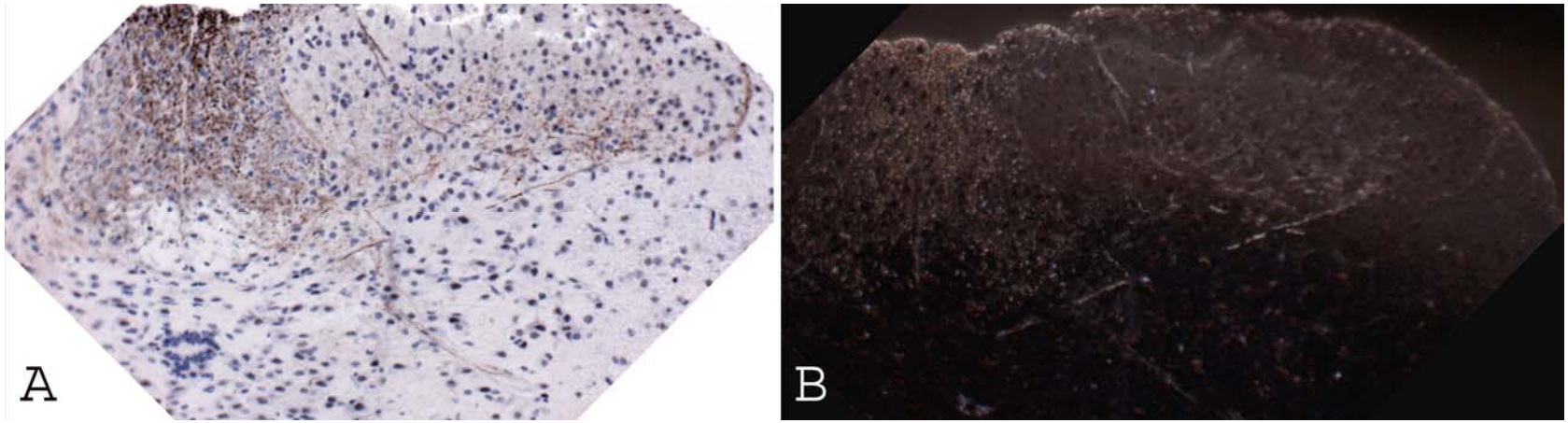

Figure 3-5 GFP immunohistochemical staining of IV day 14 spinal cord. Brown is GFP+ staining; blue is a hematoxylin counter stain. (A) and (B) are of the same section in light and dark field respectively. These pictures demonstrate the innervation of the DRG projections into the ventral grey matter of the spinal cord.

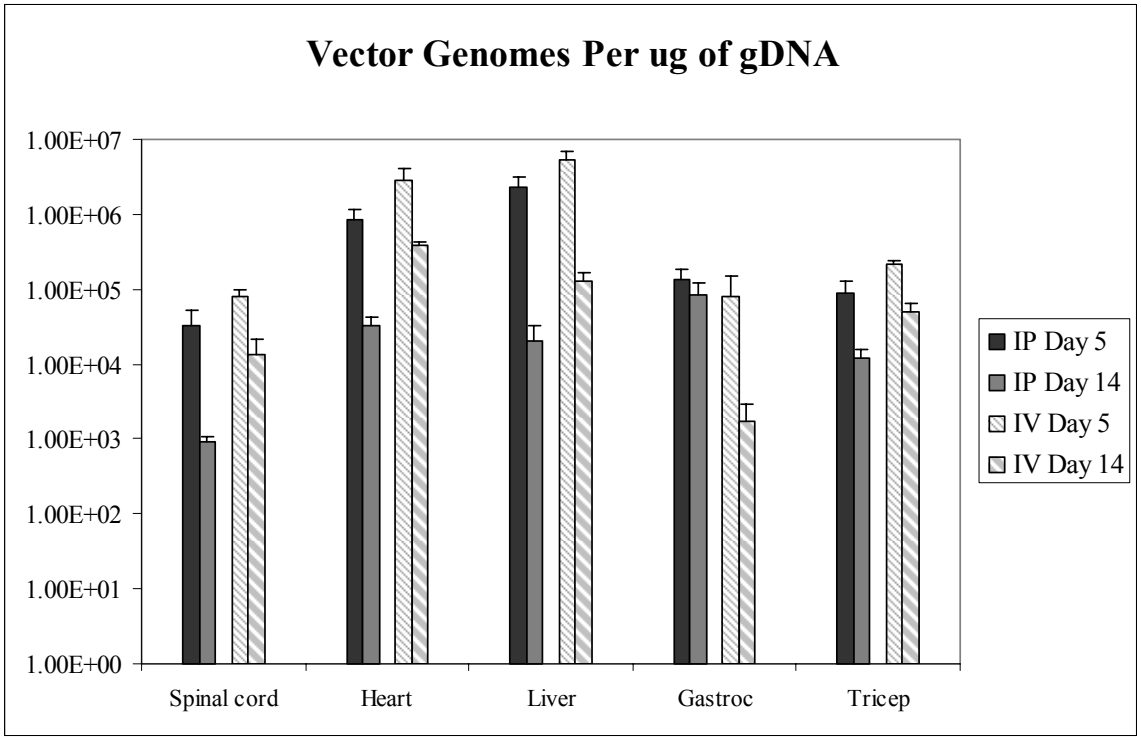

Figure 3-6 Real-time PCR results indicating the importance of survival time on vector persistence after neonate IP or IV rAAV8 injection. Only the tricep showed a significant difference between injection routes.

CHAPTER 4
ANTEROGRADE DELIVERY OF SECRETED TROPHIC FACTORS USING RECOMBINANT ADENO-ASSOCIATED VIRUS TYPE 5

Experimental Rationale

To efficiently deliver secreted trophic factors to the spinal cord we hypothesized that the anatomical relationship between the UMN and LMN could be utilized to anterogradely transport trophic factors to large areas of the spinal cord. UMN exist in defined structures within the brain and send direct axonal projections to the spinal cord where they synapse on interneurons or LMN (126). Injection of rAAV vectors into appropriate brain structures could result in sustained secretion of therapeutic trophic factors to all regions of the spinal cord with a single injection procedure.

For our proof of concept, we chose two descending motor tracts to compare which tract more efficiently anterogradely delivers trophic factors to the spinal cord. The corticospinal tract (CST) originates from pyramidal cells in the primary motor cortex. Pyramidal cells send ipsilateral axonal projections through the internal capsule, into the pyramids and decussate in medulla before proceeding to the spinal cord. In rats, the CST primarily descends contralaterally in the dorsomedial white matter. There is a small ipsilateral, ventral component which comprises 10-20% of the descending fibers. CST fibers are found in all levels of the spinal cord (129). The rubrospinal tract (RST) originates from the red nucleus that resides in the midbrain. Eighty percent of the axonal projections decussate immediately and descend contralaterally in the dorsolateral funiculus. The remaining 20% of the RST descends in the ipsilateral dorsolateral funiculus. The RST controls the proximal muscles of the upper limbs, though it has been shown to have projections to all levels of the spinal cord (130).

Results

Normal 6 week-old female Sprague-Dawley rats were injected unilaterally in either the red nucleus or the primary motor cortex. Each injection site received 3 x 10^8 viral particles of rAAV5 CB GFP or CB GDNF WPRE in a volume of 0.25µl. Due to the more diffuse nature of the motor cortex, animals received three injections while the more compact red nucleus group received one. Figure 4-1 shows a graphical representation of the rubrospinal anterograde delivery method. rAAV5 GFP animals were sacrificed at 13 weeks post injection. Examinations of spinal cords for native GFP fluorescence showed robust expression in the predicted descending tracts. Figure 4-2 shows cervical and thoracic transverse sections of spinal cords 13 weeks after unilateral RN rAAV5 GFP injection. GFP+ fibers were observed in the contralateral RST at all levels of the spinal cord examined (Figure 4-2 A-B, D and E). Unexpectedly, there were GFP+ fibers seen in the ventromedial white matter that are not part of the RST, but rather they are the ventromedial portion of CST (Figure 4-2 C). GFP+ fibers in the CST were likely the result of rAAV5 that transduced cortical projections to the RN and subsequently was retrogradely transported back to the cortex. Examination of the cortex failed to detect GFP+ cell bodies in rats. However when a similar RN injection was performed in normal mice, pyramidal cells within the cortex expressed GFP protein (Figure 4-3). Injection of the primary motor cortex in normal rats also resulted in GFP expression in the spinal cord (Figure 4-4). Examination of the cervical (Figure 4-4 A-B), thoracic (C-D) and lumbar (E-F) sections revealed GFP+ fibers descending in the dorsomedial white matter, which is the location of the contralateral CST in rodents. In high magnification sections from Ctx injected animals, axonal collaterals entering the grey matter could be observed.

In order to determine innervation of the spinal grey matter following rAAV5 GFP RN or Ctx injection, GFP immunohistochemistry (IHC) was performed on spinal cord sections. All sections examined in both groups were positive for GFP labeling. Upon low magnification examination of spinal cord sections from RN injected animals, GFP positive fibers were seen coursing through the grey matter. Dorsal horns and Rexed's lamina VII were extensively labeled. Occasional labeling in lamina VIII and IX were seen. Some fibers were seen in proximity or overlapping with neuronal cell bodies in the ventral horn (Figure 4-5 C, G). Spinal cord sections from Ctx injected animals revealed similar grey matter innervation by GFP+ fibers as seen with RN injected animals (Figure 4-6).

After rAAV5 GDNF injection in the RN, GDNF labeling in the spinal cord was similar in localization to the corresponding GFP injected animals. Labeled axons were routinely seen in the spinal grey matter (Figure 4-7). Surprisingly while GFP expression in the spinal cord following Ctx injection was easily detectable by IHC, GDNF was less apparent (Figure 4-8). The descending CST fibers in the dorsal white matter showed faint unilateral labeling, but grey matter innervation was not seen.

In order to quantify the amount of GDNF being transported to the spinal cord, GDNF ELISAs were performed on animals that had been injected in either the Ctx or RN with rAAV5 GDNF 13 weeks prior. The RN injection was significantly more efficient at delivering GDNF to all levels of the spinal cord when compared to the Ctx injected group (Figure 4-9). Also, in both Ctx and RN groups the GDNF protein levels decreased caudally. This was expected since the number of fibers comprising the descending cerebrospinal tracts normally decline as the tracts descend caudally.

Discussion

To our knowledge, this is the first use of descending motor tracts to employ anterograde transport to deliver rAAV5 derived trophic factors to all levels of the spinal cord. With a single unilateral injection procedure, GDNF was detected greater than 72mm away from the injection site at levels above background. The CNS offers a unique opportunity to deliver a small amount of virus to the brain and have its transgene product disseminated throughout the entire spinal cord. Previously, a number of groups used multiple intramuscular injections to deliver GDNF to the spinal cord in ALS mice (84, 91). Their delivery methods required ~4 x 10^{10} viral particles and a minimum of three intramuscular injections to target the spinal cord of ALS mice. In this experiment we administered 3.3 x 10^{8} viral particles, a two-log lower dose, to the much longer rat and detected high amounts of GDNF protein in all levels of spinal cord examined.

In this experiment we compared two descending motor tracts, the corticospinal and the rubrospinal tracts. The CST is the largest tract projecting to the rat spinal cord (131). It was somewhat surprising in these experiments that the RST was more efficient at delivering GDNF to the spinal cord following intracerebral injection. Both tracts were labeled well by rAAV5 GFP injection. However, via IHC and ELISA, more GDNF was detected in spinal cord after a RN injection compared to a Ctx injection. There are several potential explanations. First, GFP lacks a signal sequence and therefore is not an accurate predictor for the behavior of trophic factors in neurons. GFP detection in the spinal cord was likely from completely filling a cell with protein rather than any active transport. Second, the RN is a much smaller nucleus in the brain compared to the motor cortex. Although we administered three times the amount of vector in three separate injections to the cortex group, we likely transduced a higher percentage of the cells

comprising the RST than those of the CST. Third, the motor cortex is known to have many axonal projections within the brain. While the RN receives projections from other brain regions, its primary axonal projection is to the spinal cord.

Our brain histology shows GDNF staining in the thalamus and striatum of Ctx injected animals, known projection areas from the cortex. RN injected animals also have GDNF staining in the striatum, but that is probably due to incidental nigrostriatal transduction at the injection site. Assuming there is no preference or bias from which axonal collateral GDNF is secreted, it is likely that the majority of GDNF protein made in the RN is secreted in the spinal cord while the motor cortex likely subdivides its GDNF secretion among its many projections.

Numerous studies have used trophic factors to treat ALS animal models and pateints. Repeated intracerebroventricular (ICV) administration of VEGF to ALS rats delayed disease onset by 17 days and improved survival by 22 days (107). This treatment regimen required daily ICV injections of recombinant VEGF starting at 60d of age. Intrathecal infusions of IGF1(100 mg/kg daily) delayed onset by ~34 days and improved ALS mouse survival by ~29 days (104). Recombinant protein delivery was also used in clinical trials of ALS patients, but had little success due to the short half-lives of the proteins delivered. The animal studies are invaluable to demonstrate efficacy of trophic factors, but the clinical studies emphasize the need for a continuous delivery method. Gene transfer using viral vectors has been shown to provide sustained secretion of trophic factors in a number of animal studies, including studies in ALS animals (84, 91, 101, 132-134). Preclinical studies used intramuscular injections of adenoviral or AAV vectors to treat ALS mice and had great success. There are two reasons why the

anterograde delivery may be superior to intramuscular delivery. First, in humans, IM delivery would likely require hundreds of injections and large amounts of virus to deliver trophic factor to the entire spinal cord. Multiple injections increases the chance of immunological reactions at the injection sites and/or to the high titer of virus administered. Second, upper motor neuron degeneration has been shown in ALS (135). Anterograde delivery can potentially include UMN in the treatment while intramuscular delivery fails to treat the UMN directly. Anterograde delivery would require a more invasive injection procedure when compared to IM injections, but would require far less virus to potentially reach the entire spinal cord.

Intracerebral injection of viral vectors may have uses beyond neurodegenerative diseases. Anterograde delivery of trophic factors may aid in the survival of tissue grafts, could provide growth promoting factors or suppress local inhibitory cues after spinal cord injury. Another implication of the anterograde delivery route of rAAV derived GFP is its utility in long tract tracing. rAAV GFP expression can be maintained at high levels for the life of the animal. There is no chance of GFP leakage as with some dyes; or of trasferring across the synapse as with lectins. GFP can be visualized without any histochemical labeling, and therefore can be used in cell culture or living tissue (136). Our study shows rAAV GFP's ability to completely fill the cytoplasm and projections of neurons allowing for easy, long term visualization.

Finally this study emphasizes the potential hazards of gene therapy in the CNS. The interconnectivity of the CNS limits the concept of a localized treatment. For example, our injection sites in the primary motor cortex were designed to deliver GDNF to the spinal cord. Figure 4-10 (A-C) clearly shows that restricting secretion to one

projection field or another is not possible with the current technology. Our cortex injections resulted in abundant GDNF expression in the striatum and thalamus. Although we didn't examine the cerebellum, uptake and retrograde transport of virus by the cerebellorubral projections following red nucleus injection is also a possibility. However, when facing an unrelenting terminal disorder such as ALS there may be a greater allowance for potential side effects.

In conclusion, we have demonstrated the ability of rAAV5 to anterogradely deliver GDNF to all levels of rat spinal cord following a single intracerebral injection procedure. Hopefully this new delivery method can aid in translational and basic science endeavors in the spinal cord.

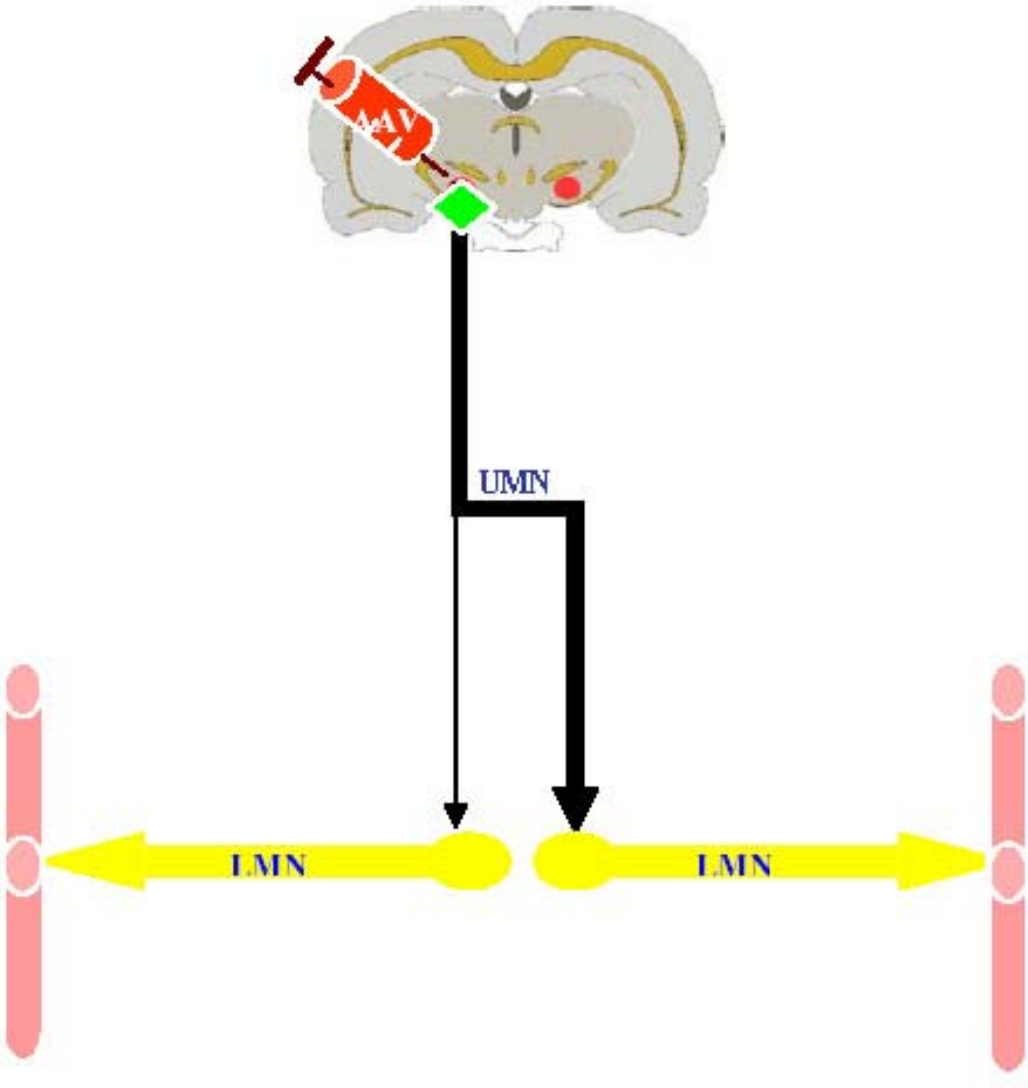

Figure 4-1 Schematic representation of a unilateral rAAV injection in the red nucleus. The black arrows represent the descending axons that originate from the red nucleus. The relative thickness of the arrows shows ipsi- and contralateral components of the RST. Ideally, the UMN synapse directly on the LMN (yellow) in the spinal cord. The LMN project out from the spinal cord and synapse on skeletal muscle (pink).

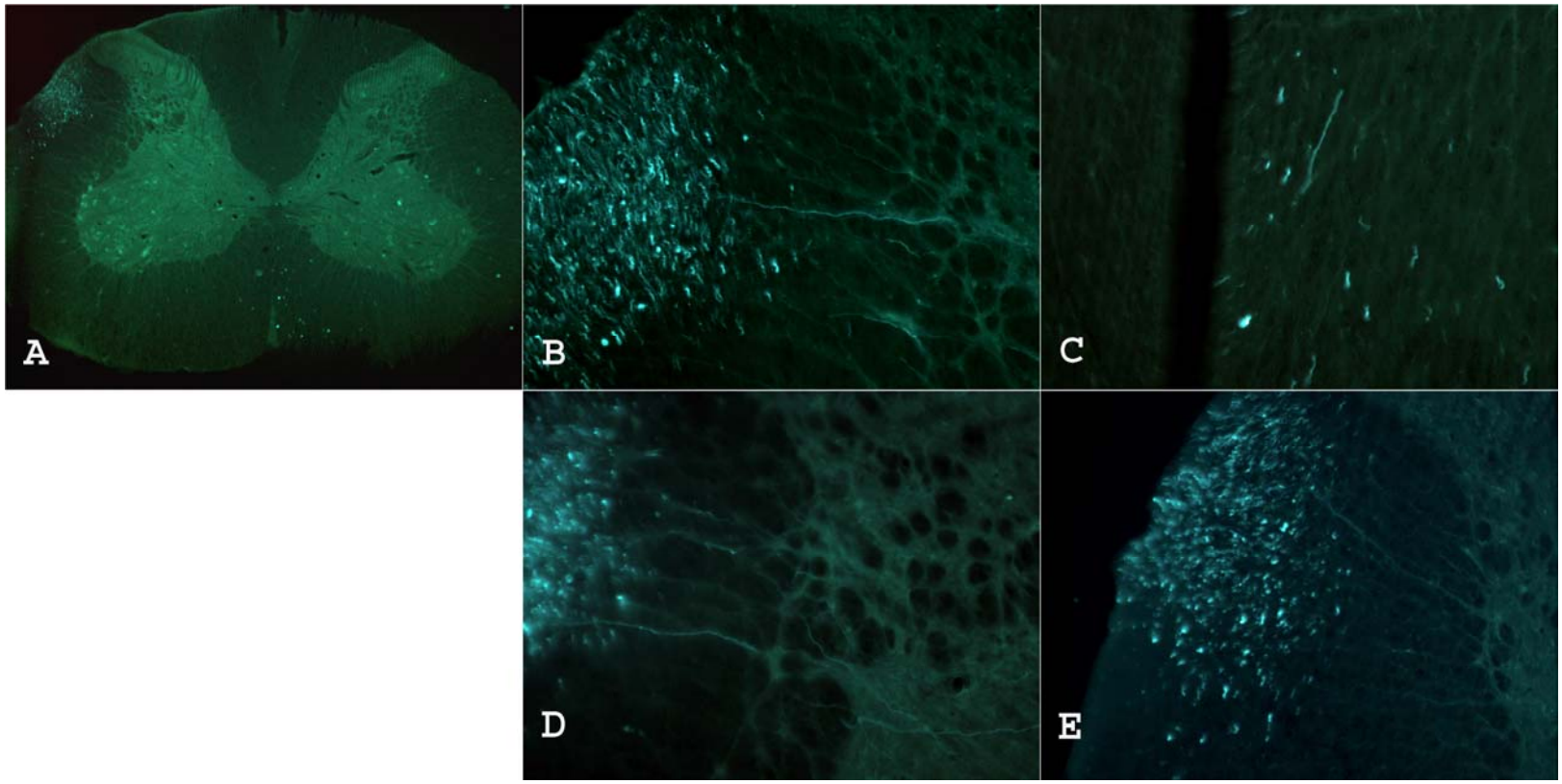

Figure 4-2 Native GFP fluorescence in the cervical (A-C) thoracic (D) and lumbar (E) levels of spinal cord 13 weeks after a unilateral rAAV5 GFP red nucleus injection. (A) A low magnification picture of transverse section through the high cervical cord. GFP positive fibers are visible in the contralateral RST and ipsilateral CST. (B) The contralateral portion of the RST in cervical spinal cord. The green dots in the dorsolateral funiculus are descending fibers exiting the plane of the page. (C) The ipsilateral component of the CST. (D) The contralateral RST in thoracic spinal cord. (E) Contralateral RST in lumbar spinal cord.

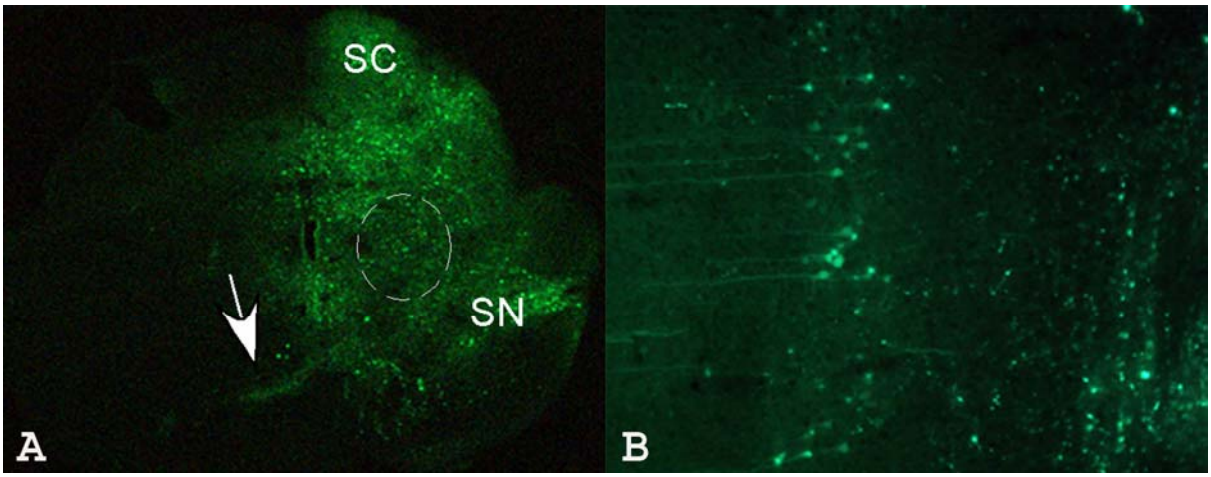

Figure 4-3 Native GFP fluorescence in a mouse brain after rAAV5 GFP injection into the red nucleus. (A) shows the unilateral injection site. The circle denotes the red nucleus. The arrow is pointing to decussating fibers of the RST. There is also incidental transduction of the SC and SN. (B) shows pyramidal cells from the cortex of the same animal. This suggests a retrograde transport of the viral vector by cortical projections from the site of injection to the cell bodies. SC = superior colliculus SN = substantia nigra

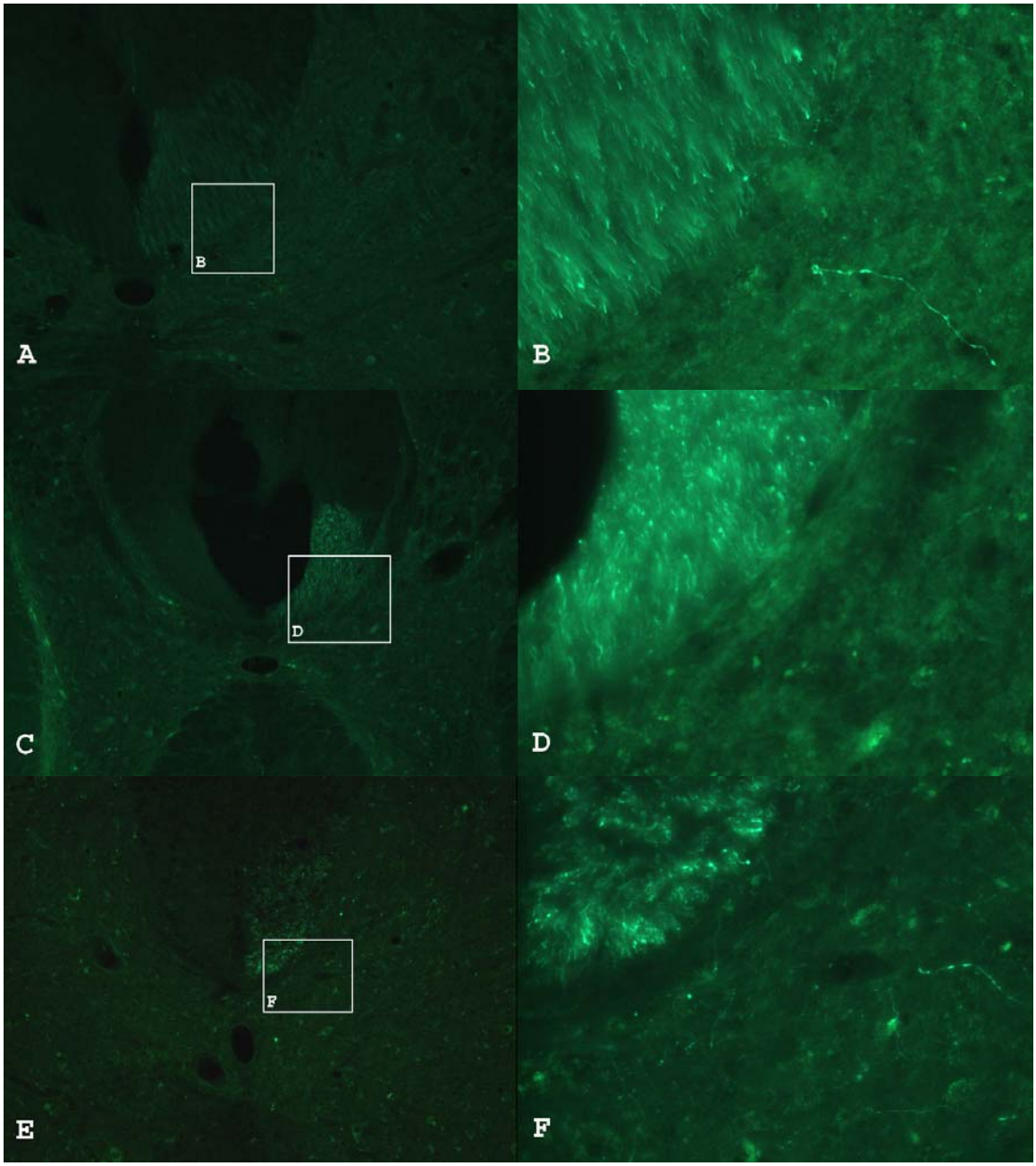

Figure 4-4 Cervical (A-B), thoracic (C-D) and lumbar (E-F) transverse sections through the spinal cord of a rat that received a unilateral motor cortex injection of rAAV GFP. CST transduction is seen in the dorsomedial white matter in cervical, thoracic and lumbar sections in (A), (C) and (E) respectively.

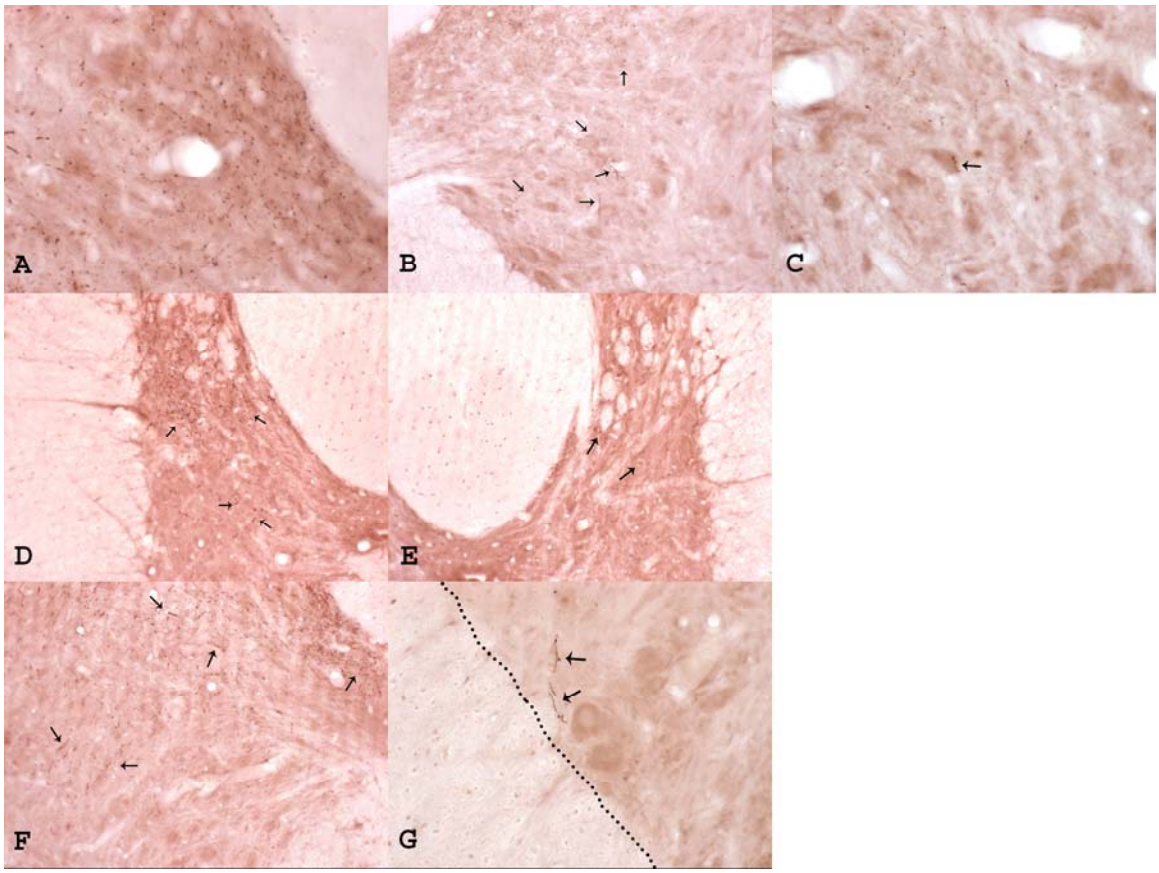

Figure 4-5.GFP IHC 13 weeks after unilateral rAAV5GFP injection in the RN. Positive staining is indicated by brown dots or lines throughout the grey matter. (A) The dorsomedial grey matter contralateral to the RN injection in cervical spinal cord. GFP labeled fibers were seen throughout the grey matter. (B) GFP labeled fibers were seen ipsilateral to RN injection in cervical spinal cord. (C) Labeled GFP fiber in cervical spinal cord overlapping a cell body. (D and E) Contralateral and ipsilateral respectively RST labeling of the spinal grey matter in thoracic sections of the spinal cord. (F) GFP labeled fibers were visible in the grey matter of lumbar sections after RN injection. (G) Labeled GFP fibers in lumbar spinal cord in close proximity to ventral horn neurons.

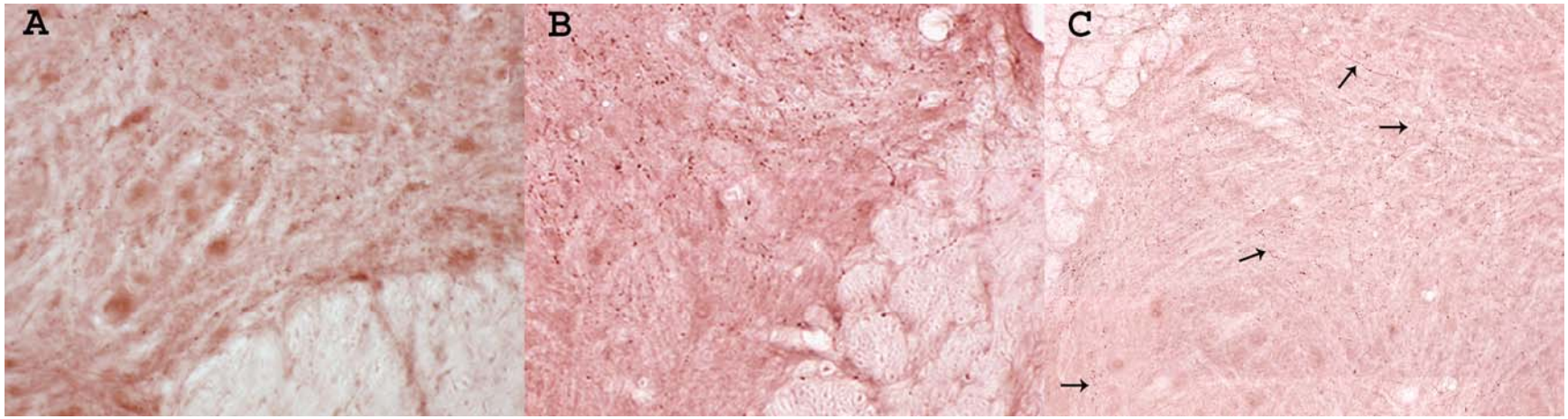

Figure 4-6 GFP IHC in the cervical (A), thoracic (B) and lumbar (C) levels of the spinal cord following a unilateral injection of the motor cortex with rAAV5 GFP. (A) and (B) positive staining has the appearance of brown dots scattered throughout the grey matter. (C) The arrows indicate GFP+ axons in the grey matter of lumbar spinal cord. This section is approximately 65mm away from the site of injection. All sections were examined at 13 weeks post injection.

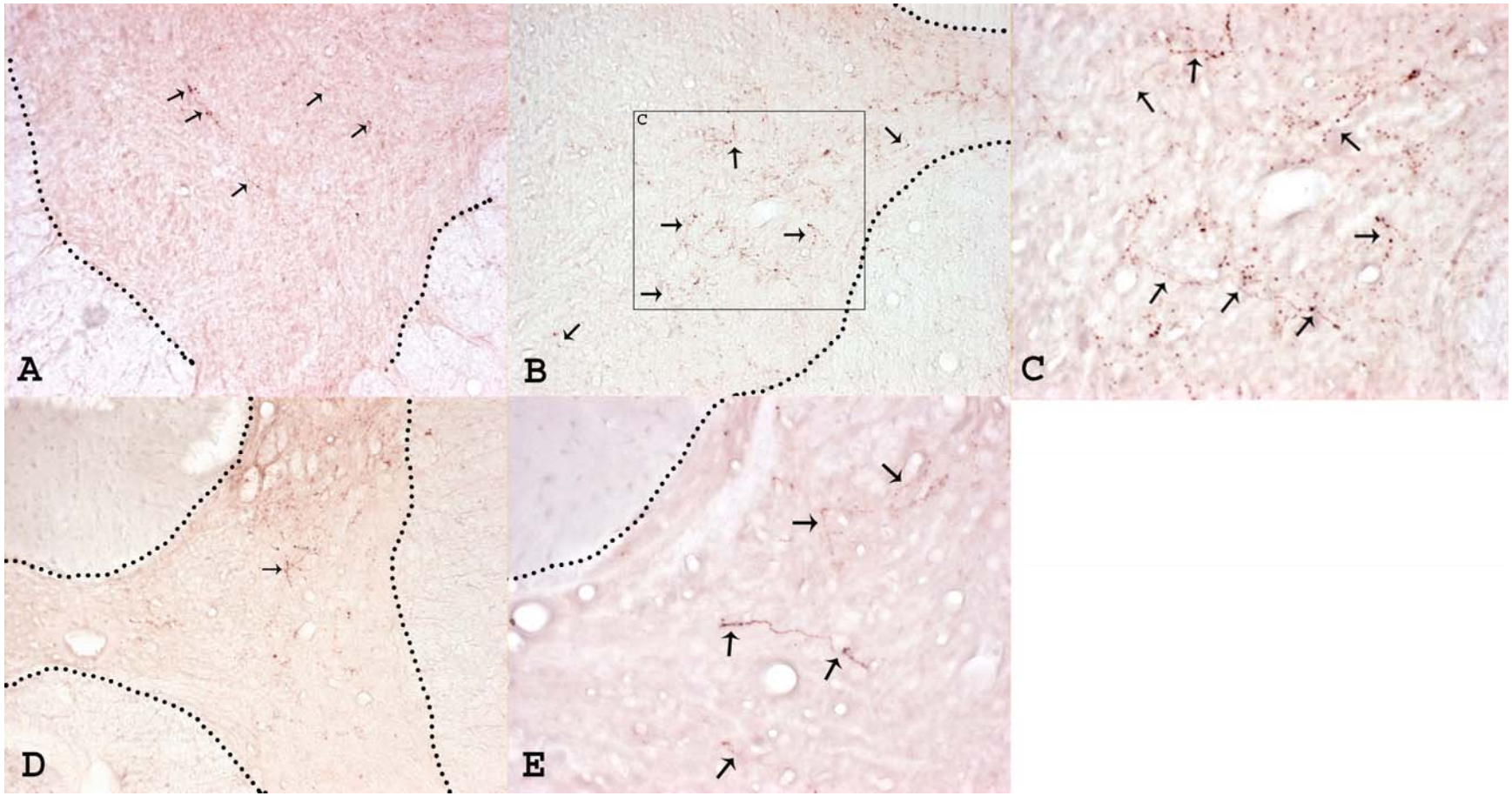

Figure 4-7 GDNF IHC in various levels of the spinal cord 13 weeks after rAAV5 GDNF injection into the RN. (A) The arrows denote labeled axons in the spinal grey matter ~6 mm caudal to the brain. (B) and (C) show GDNF positive axons in the spinal grey matter ~18 mm caudal to the brain. (D) and (E) again show GDNF positive axons in the spinal grey ~42 mm caudal to the brain. Arrows are indicating GDNF+ axons while the dotted lines demarcate the grey-white border in the spinal cord.

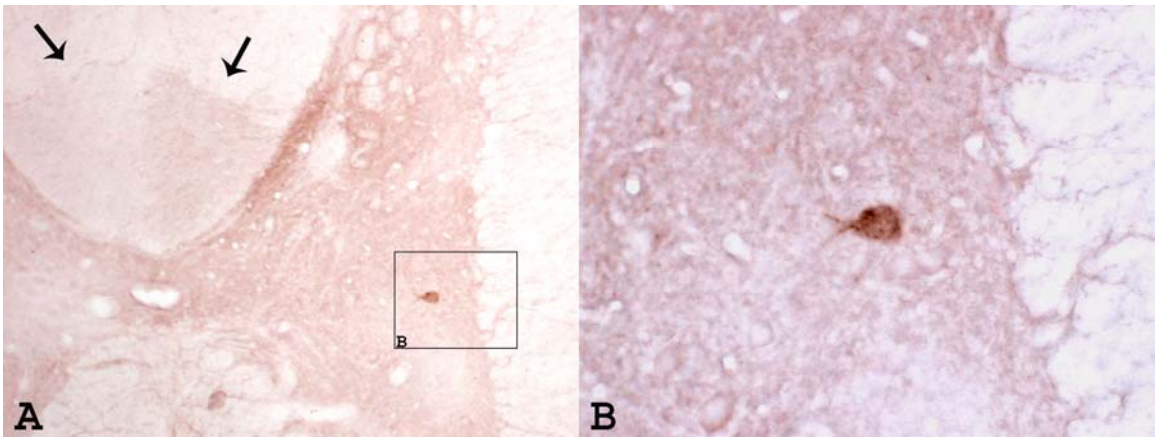

Figure 4-8 GDNF IHC in thoracic spinal cord 13 weeks after rAAV5 GDNF unilateral injection in the motor cortex. GDNF+ fibers innervating grey matter were rarely seen. However the dorsal CST showed a consistent difference between uninjected and injected sides (A, arrows). (B) shows a GDNF labeled cell from the same section.

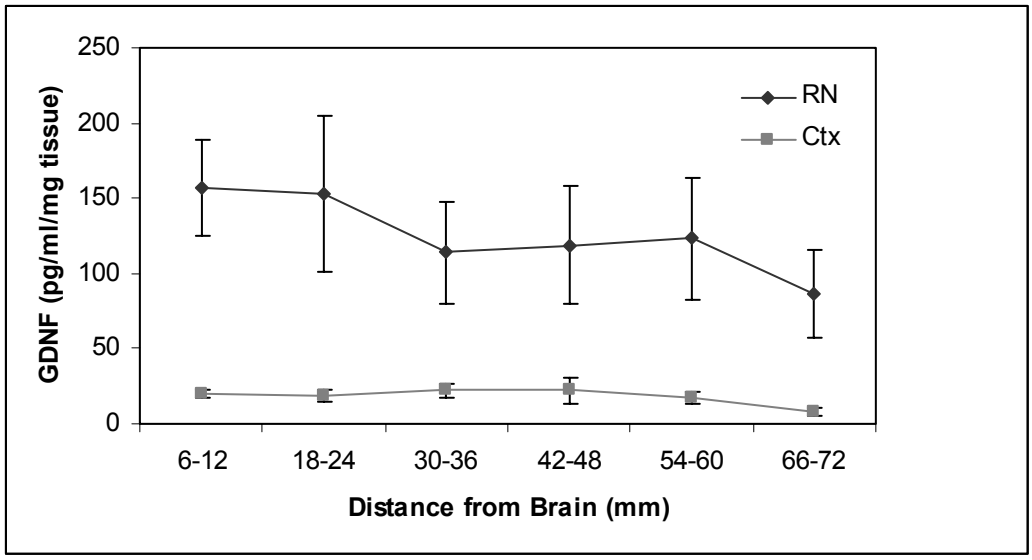

Figure 4-9 GDNF levels in spinal cords of animals unilaterally injected with rAAV5 GDNF into either motor cortex (Ctx) or red nucleus (RN). Animals were sacrificed 13 weeks post injection, and spinal cords were harvested for analysis. Differences in GDNF values at each spinal cord level were statistically significant $F(5,35) = 2.68$ ($p = .034$)

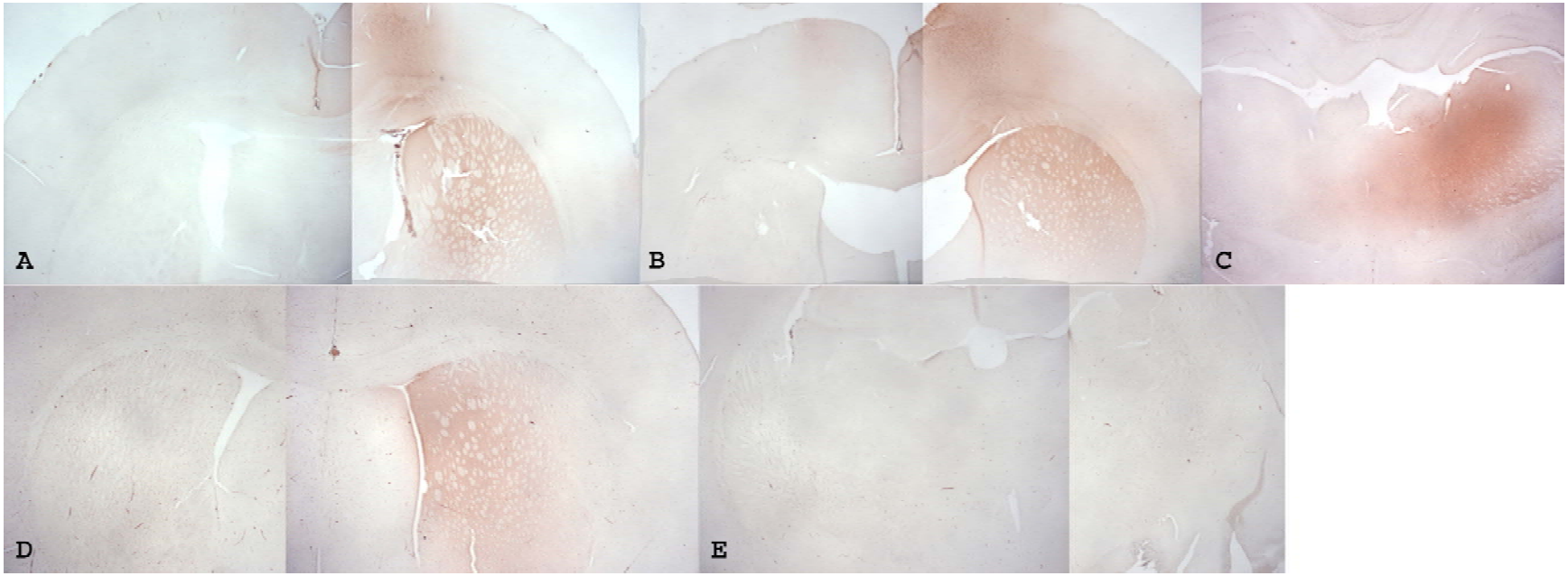

Figure 4-10 GDNF IHC in uninjected structures throughout the brain. (A), (B) and (C) shows GDNF protein in the striatum (A and B) and thalamus respectively 13 weeks after rAAV5 GDNF motor cortex injection. (D) and (E) shows GDNF protein in the striatum and absence of staining in the thalamus 13 weeks after rAAV5 GDNF injection in the RN. GDNF secretion into striatum after RN injection is likely due to incidental substantia nigra transduction when targeting the RN.

CHAPTER 5
RECOMBINANT AAV5 GDNF INTRACEREBRAL INJECTION TO TREAT ALS RATS

Introduction

Amyotrophic Lateral Sclerosis (ALS) is an adult onset degenerative neuromuscular disease. Lower motor neurons (LMN) and upper motor neurons (UMN) are both affected in ALS (135). Recently a number of transgenic animal models were created using genetic mutations in the Cu/Zn SOD1 gene (137). SOD1 mutations are responsible for a small percentage of the overall ALS patient population, but these animal models accurately mimic physiological and pathological defects of both sporadic and familial cases of ALS. With the advent of the ALS models came improved understanding of disease progression. Perhaps more importantly, these models give an arena to explore potential therapies.

For this study we chose a commercially available transgenic rat model. The $SOD1^{G93A}$ ALS model is constructed on a normal Sprague-Dawley rat background (35). These rats show 8 fold over expression of the human $SOD1^{G93A}$ transgene at a pre-symptomatic stage; which increases to 16 fold at end stage of disease. Disease onset occurs at approximately 115 days old. The first symptoms are abnormal gait or hindlimb weakness. Disease progression is rapid (an inability to right themselves when placed on their side) 11 days after onset. Severe muscle atrophy, immobility and loss of grooming are all evident at endstage. Spinal cord examination in pre-symptomatic animals shows vacuoles forming in the ventral neuropil prior to LMN loss. There is no evidence of neuropil vacuolization in endstage G93A rats. Also at endstage there is LMN axon and cell body loss as seen by ventral root and horn staining. The G93A rat also has a reduction in the astrocytic glutamate transporter EAAT2 at endstage. Finally, ALS rats also demonstrate protein aggregates, another hallmark of ALS disease pathology, which are immunopositive for SOD1, Hsc70, ubiquitin and neurofilament (35). The rat model is also

superior to the mouse model in that it allows for more diagnostic behavioral testing to better assess disease onset and progression. In summary, mutant SOD1 transgenic rats possess many of the characteristics of ALS in humans.

GDNF has long been recognized as an important trophic factor for healthy and injured LMN (138). Because of this, many groups have used viral vector derived GDNF to treat ALS mice. Two groups (84, 139, 140) used Adenoviral vectors injected in the muscle to partially rescue LMN in different mouse models of ALS. Acsadi slowed disease progression and increased survival in affected mice after GDNF treatment. Similar results were also seen with rAAV2 derived GDNF (94). rAAV2 GDNF injected into muscle of all four limbs delayed disease onset in G93A mice, and favorably shifted the size distribution of LMN when compared to untreated controls. Together, these results show that rAAV derived GDNF can have therapeutic benefit in treating ALS mice. The Wang study was performed in mice with the same transgene (G93A) as the transgenic rats described above.

All of the GDNF gene therapy studies used intramuscular injections of viral vectors to deliver their therapy to LMN. When scaled up to a human, intramuscular gene therapy could require hundreds of injections and large amounts of virus before exacting therapeutic benefit. Our study sought to capitalize on the anatomical relationship between UMN and LMN by delivering our rAAV GDNF gene therapy to the red nucleus (RN). The RN is a small nucleus in the midbrain that is the origin of the rubrospinal tract (RST). The RST is a motor tract that primarily sends contralateral projections down the spinal cord to synapse on interneurons or directly on LMN in the ventral grey matter (130, 141). The RST is responsible for controlling the large muscles of the arms. Rescue of LMN innervated by these cells could provide a drastic improvement allowing for use of the upper limbs. In a rat this could aid in feeding, movement

and grooming. Additionally, the RST could secrete trophic factor at the level of the phrenic motor pool, thereby preserving diaphragmatic innervation and ameliorating respiratory problems (142). Late stage ALS patients require mechanical intervention to breathe. Inability to breathe independently is ultimately the cause of death in ALS patients.

Results

Presymptomatic 8 week old female ALS rats and their WT littermates were bilaterally injected with 1 x 10^9 particles of rAAV5 CB GDNF WPRE or rAAV5 CB GFP. GFP injections acted as controls for rAAV injections within the red nucleus, and have not previously been shown to impact any of our outcome measures. The volume of vector delivered to each RN was 0.25µl. Interestingly, at the date of surgery there was already a difference in body weight between ALS and WT rats ($p=0.008$). Eight weeks of age was prior to any physical symptoms of ALS and may indicate a subclinical level of early pathology. All animals were tested for gait analysis and cylinder rearing tests prior to and 5 weeks post surgery.

In cylinder rearing tests (Figure 5-3), animals were given 5 minutes of free spontaneous activity in a clear plexiglass cylinder in a darkened room. Sessions were videotaped and scored for number of rears (both front limbs leaving the floor). This activity is highly dependent on the hind limbs. The cylinder rearing tests performed at 5 weeks post injection (13 weeks of age, prior to symptom onset) showed no difference between GDNF and GFP treatments. However this test has not previously been used for ALS rats. When the rearing data was analyzed across genotype a trend showing a difference was noted $F(1,14) = 3.94$, ($p = 0.067$).

To assess changes in gait, foot print analysis was performed prior to (8 weeks of age) and 5 weeks post surgery (13 weeks of age). Front and hind foot pads were coated with two separate colors of non-toxic paint. The animals were then put in a clear plexiglass corridor in which the

floor had been lined with receipt tape. The animals proceeded down the corridor to a darkened goal box while their foot prints were recorded on the receipt tape. Measurements of stride length and width for both front and hind limbs were recorded. Only front stride length was different between GDNF and GFP ($p = 0.008$) (Figure 5-4). As with cylinder rearing, the analysis was repeated across genotype. Both front and rear stride lengths were significantly longer in ALS animals compared to wild type littermates $F(1,8) = 6.48$ ($p = 0.035$) and $F(1,8) = 24.66$ ($p = 0.001$) respectively.

There was no difference in survival between GDNF (126.5d +/- 3.1) and GFP (130.4d +/- 3.1) treatment $F(1,9) = 0.783$, ($p = 0.40$). RST GDNF over expression in rats induced a significantly lower body weight (Figure 5-1) than GFP treated ALS rats ($p = 0.03$). Both ALS groups were significantly different than wild-type litter mates ($p<0.001$ for both treatments). Histology (Figure 5-2) confirmed rAAV targeting of the RN and subsequent protein expression and transport to the spinal cord. GDNF staining was seen in the midbrain and at all levels of spinal cord examined.

To test whether the GDNF had any effect on LMN, we labeled spinal cord sections for calcitonin gene related peptide (CGRP) expression in wild type and end stage ALS animals. CGRP labels the superficial dorsal horn and LMN specifically. CGRP labeling intensity has also been shown to increase in response to GDNF (143). Stereological counts of CGRP+ LMN at levels C3-C5 from endstage animals showed no difference between GDNF and GFP treated animals ($p = 0.71$) (Figure 5-5). Additionally, there was no noticeable difference in CGRP labeling of LMN between GFP control and GDNF treated groups (Figure 5-6).

Discussion

After bilateral RN rAAV5 GDNF or GFP injections, transgene expression reached all levels of the spinal cord. Even though GDNF was dispersed throughout the spinal grey matter,

no improvements in ALS symptoms could be detected. rAAV5-GDNF injected ALS rats lost weight compared to GFP injected ALS rats (Figure 5-1). These data demonstrate that there was a clear physiological effect of GDNF expression. GDNF mediated weight loss is probably the result of hypothalamic GDNF expression due to the RN's proximity to the hypothalamus. rAAV GDNF injections in the hypothalamus have previously been shown to induce weight loss in rats (144-146).

The advantage of a rat model over a mouse is the ability to easily perform behavioral tests which can serve as additional outcome measurements in studies testing potential therapies. The cylinder rearing test, derived from the paw-touching tests performed on hemi-lesioned Parkinson's rats (134), relies on exploratory behavior and hind limb strength to assess disease progression in pre-symptomatic ALS animals. Although the cylinder test failed to detect any difference in treatments in our experiment, ALS rats tended to rear less often than wild-type litter mates. Gait analysis revealed that front stride length was different between treatments (Figure 5-4 A). Together these data validate the use of cylinder rearing and gait analysis to assess disease progression in the (G93A) ALS rat.

The lack of efficacy from centrally delivered GDNF is in stark contrast to the therapeutic benefit observed in other studies that administer GDNF in the periphery (84, 139, 140). Two possibilities could explain these results: Differential expression of the GDNF receptor complex or the muscle having a role in ALS pathology. GDNF receptor expression (GFRα1) was reduced in ALS mouse muscle. GFRα1 expression in spinal cords of normal animals is down regulated in adulthood. GFRα1 down regulation is accelerated in G93A mice (147). However Mitsuma, et al. (148) found mRNA of RET (a GDNF co-receptor important for signaling) was reduced in ALS patient spinal cords while GFRα1 mRNA was unchanged. It is important to

note that Mitsuma's patient tissue was obtained from patients with idiopathic ALS. Differences in causes of ALS may play a role in differential GDNF receptor expression. Regardless, both studies indicate decreases in components of the GDNF receptor complex in the spinal cord. In the muscle, GDNF receptor levels remain constant through disease progression while GDNF mRNA expression decreased at endstage in ALS patients (149).

Recent work shows that centrally derived GDNF fails to rescue LMN in models of ALS (101, 150). In a clever experiment, Li, et al. crossed mice with a GDNF transgene under the control of an astrocyte or muscle specific promoter to ALS mice. Astrocyte controlled GDNF expression failed to improve disease onset, progression or survival while muscle derived GDNF improved all three including LMN counts versus age matched controls (150).

The down regulation of GDNF receptor expression in ALS spinal cords coupled with the need for muscle inclusion for GDNF efficacy in ALS animals, raises the question of where muscle derived factors exert their positive effects. Miller, et al. addressed the importance of muscle in ALS mice with three experiments (151). The conclusion Miller reached was that muscle is not a target in ALS.

A different trophic factor may be effective utilizing antrograde delivery to the spinal cord. Insulin-like growth factor 1 (IGF1) was shown to be therapeutic in animal models of ALS following intrathecal administration of recombinant IGF1 (104) or intramuscular injection of rAAV2 expressing IGF1 (91). Importantly, intramuscular injection of a viral vector expressing IGF1 required that the vector be able to undergo retrograde transport to attain maximum efficacy (91). Recombinant IGF1 is in phase III clinical trial to treat ALS (152). The effectiveness of IGF1 in treating ALS mice after intrathecal administration suggests the anterograde delivery of IGF1 from UMN to the spinal cord may also be effective.

Recombinant vascular endothelial growth factor (VEGF) showed efficacy in ALS rats using repeated intracerebroventricular (ICV) injection (107). This group also showed anterograde transport of the ICV administered radioactively labeled VEGF by ligating the sciatic nerve. Moreover, labeled VEGF accumulated on the spinal cord side of the ligation. To support the claim of anterograde transport, axonal transport blockers prevented accumulation of VEGF at the ligation. Additionally the anterograde transport of VEGF increased the number of NMJ that were innervated in ALS rats at disease onset. This NMJ improvement may indicate a transcytosis (127) of anterograde transported trophic factors.

Inherent in the anterograde delivery is a belief that the GDNF seen in the labeled axons of the spinal cord is secreted. Lack of any measurable effect in the spinal cord leaves the possibility that GDNF is not escaping the presynaptic axon. When the same rAAV5 CB GDNF WPRE construct is unilaterally injected the substantia nigra, the nigra-striatal projections fill the striatum with GDNF. In nigrostriatal GDNF over expression, GDNF appears to be distributed extracellularly in a cloud like staining pattern (134). Some evidence of a similar GDNF staining pattern was observed in spinal cord sections from animals that received rAAV5 GDNF injections in the RN (Figure 5-7). In the context of the nigrostriatal projections, the secreting axons are projecting to a more anatomically defined space which could allow for better visualization of the accumulated GDNF. Conversely, the RST has been shown to project to all levels of the rat spinal cord thereby spreading its GDNF production over ~70mm of tissue (130). Also, there were GDNF+ cells in the dorsal horns and medial grey matter at C3 of the spinal cord after RN injection. One possible interpretation of these labeled cells is postsynaptic uptake and labeling of GDNF. However, the GDNF+ cells in the spinal cord were in areas that others have labeled by retrograde tracers injected in the periacqueductal grey area of the midbrain (153). This region

is very near the RN and could be exposed to virus during our injection procedure. It is noteworthy that no labeled cells were seen in the spinal cord after rAAV5 GFP RN injections. Utilization of a GDNF-GFP fusion protein may help demonstrate axonal secretion by indicating extracellular localization of the normally cytoplasmic GFP.

Since human GDNF cDNA was used in the rAAV vectors, there may also be immunological considerations regulating GDNF detection in the spinal cord. Inflammatory responses including activated microglia and increased COX-2 expression have been shown in ALS animal spinal cords (154). Moreover, GDNF has been shown to regulate aspects of activated microglia behavior (155). Although shown to be biologically active in studies within the Mandel lab and this study (Figure 5-1), it is possible that introduction of a non-self protein into the heightened inflammatory state of the ALS spinal cord could hasten GDNF clearance.

In conclusion, GDNF application for treating ALS is highly dependent on application in the periphery to exact its therapeutic benefit. Going forward with the anterograde delivery route to treat ALS likely requires changing the therapeutic transgene to one that has been shown to have benefit after spinal cord administration such as IGF1.

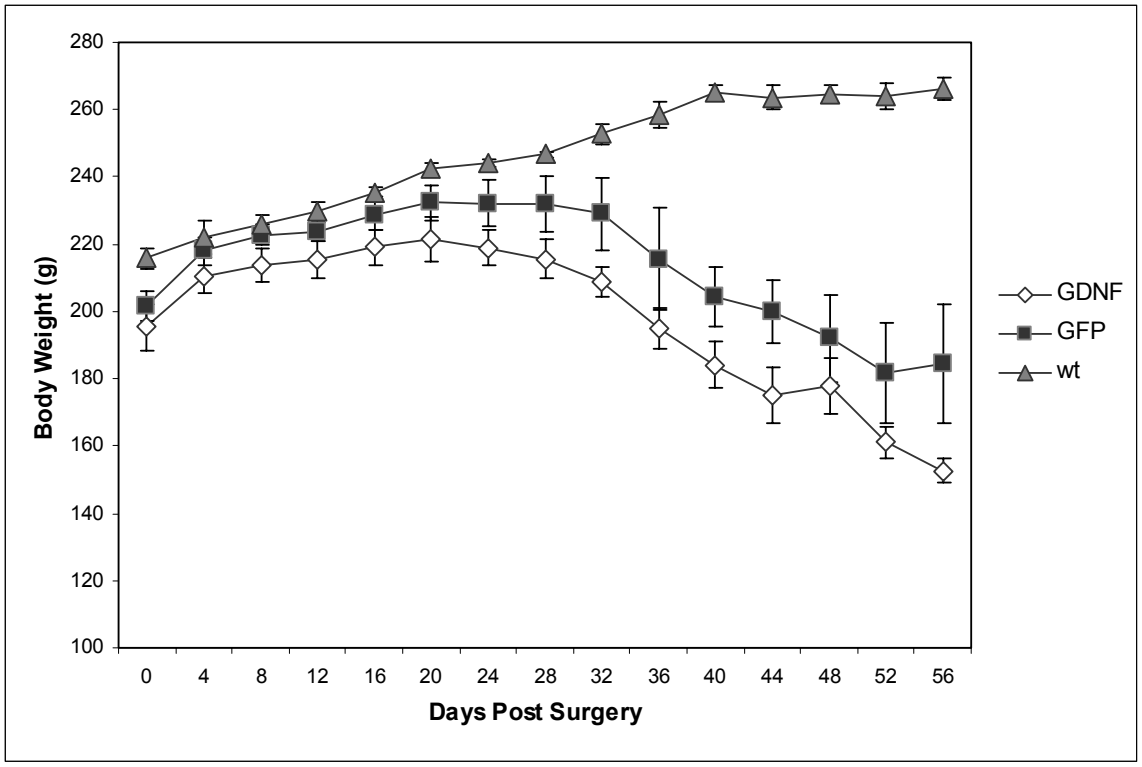

Figure 5-1 Body weight over time of rAAV5 GDNF or GFP treated ALS rats in comparison to wild-type litter mates. GDNF animals showed significantly lower body weights from GFP animals ($p = 0.032$). GDNF has been shown to reduce body weight in normal rats. This shows the rAAV5 produced GDNF has a biological effect.

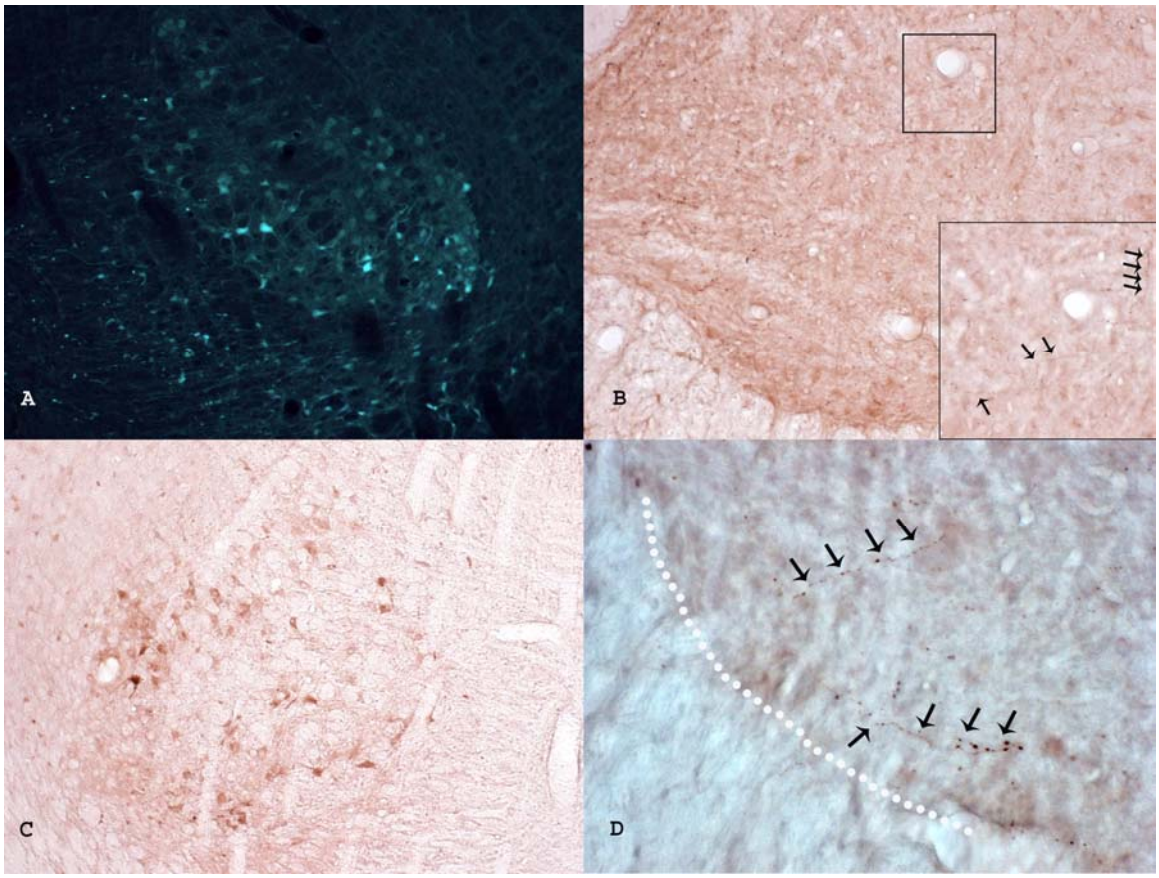

Figure 5-2 Histology from ALS animals verifying proper red nucleus injections. In B-D, the red/brown color indicates positive labeling of GFP or GDNF. (A) shows native GFP fluorescence of the red nucleus. (B) Shows a transverse cervical section through the spinal cord of a RN rAAV5 CB GFP injected animal. The inset shows high magnification of the GFP labeling. The arrows indicate UMN axon collaterals moving through the spinal cord grey matter. (C) Shows a coronal section through the RN of a rAAV5 CB GDNF WPRE injected animal. (D) shows high magnification of a transverse section through cervical spinal cord of an rAAV5 CB GDNF WPRE injected animal. The white dashed line indicates the border between the ventromedial white matter and the ventral grey matter. The arrows indicate GDNF positive labeled axons within the ventral grey matter.

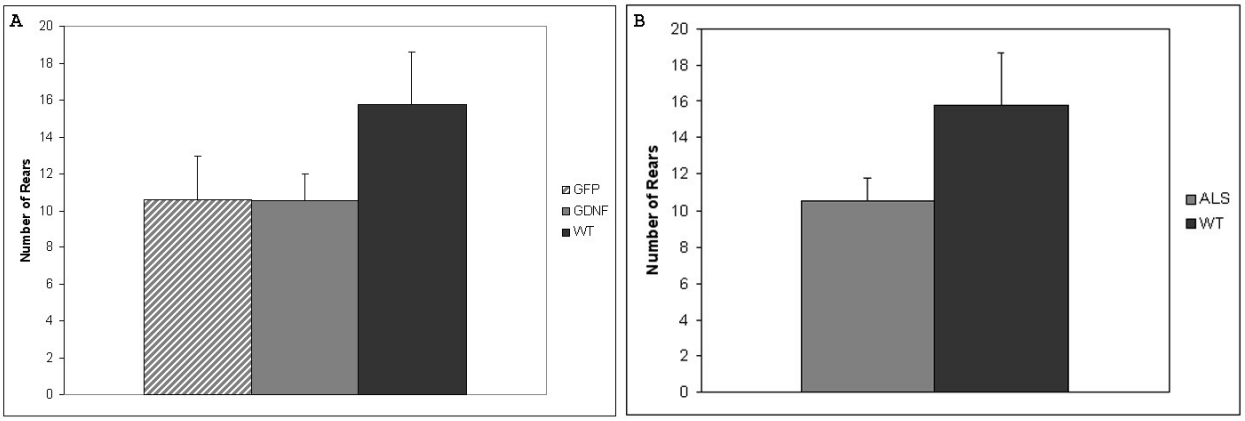

Figure 5-3 Cylinder Rearing (A) Cylinder rearing at 13 weeks shows no difference between GDNF and GFP treatment ($p = 0.97$). (B) The same data in (A) compared across genotype. There is a trend ($p = 0.067$) showing a difference in spontaneous rearing at 13 weeks of age.

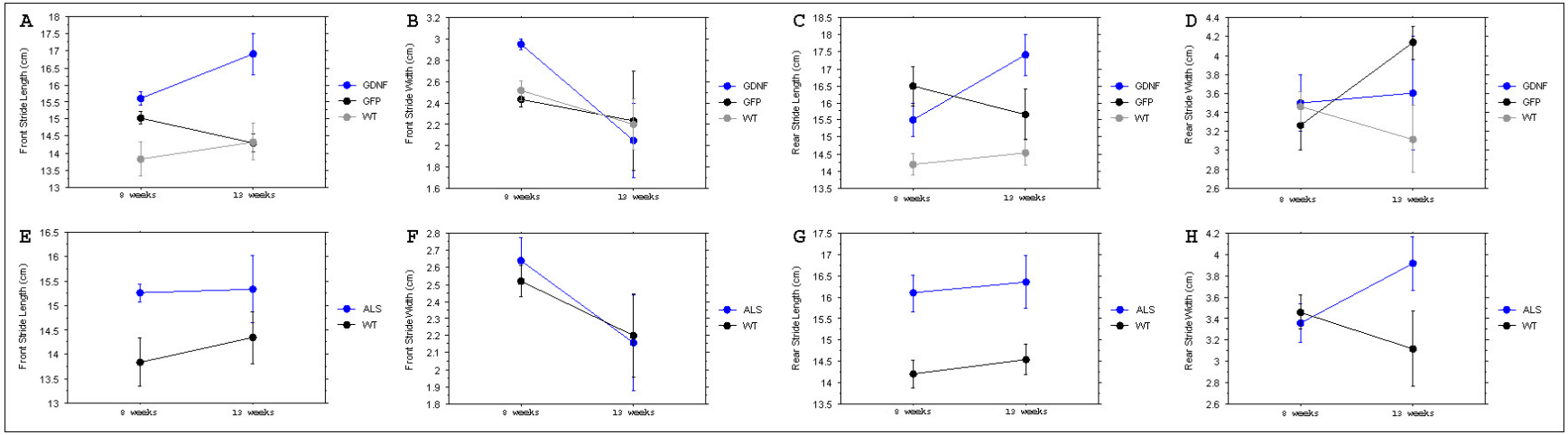

Figure 5-4 Gait analysis of rAAV GDNF, GFP and wild type littermates at 8 and 13 weeks of age. The 8 week time point is at the time of injection. The 13 week time point is prior to limb paralysis. Only Front Stride Length (A) showed a significant difference between GDNF and GFP treatments ($p = 0.008$). (E-H) shows the same data in panels (A-D) analyzed for animal genotype. Significant differences were obtained between ALS and WT animals for Front Stride Length (E) ($p = 0.035$) and Rear Stride Length (G) ($p = 0.001$). In both measurements ALS animals showed longer stride lengths than wild type littermates.

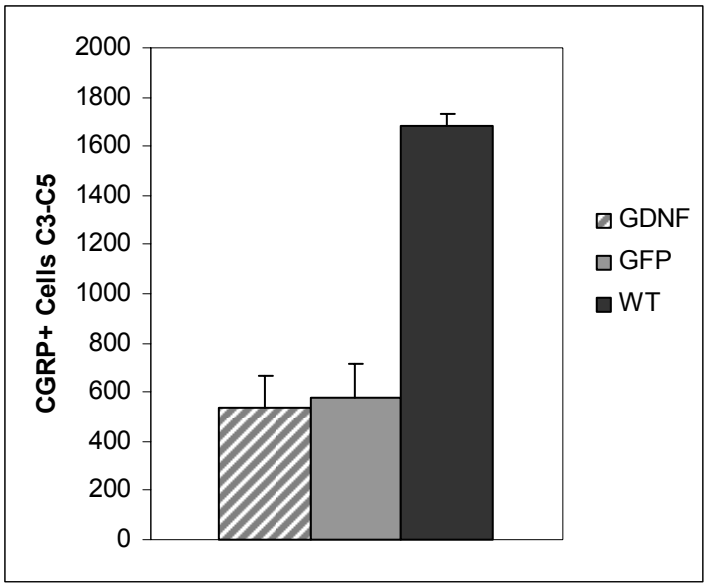

Figure 5-5 Stereological estimation of CGRP+ cells from cervical spinal cord from end stage ALS rats and wild type litter mates. CGRP is a motor neuron marker. There was no difference between GDNF and GFP treatments in rescuing lower motor neurons in C3-C5 ($p = 0.71$). Both GDNF and GFP were significantly different than wild type animals ($p < 0.0001$)

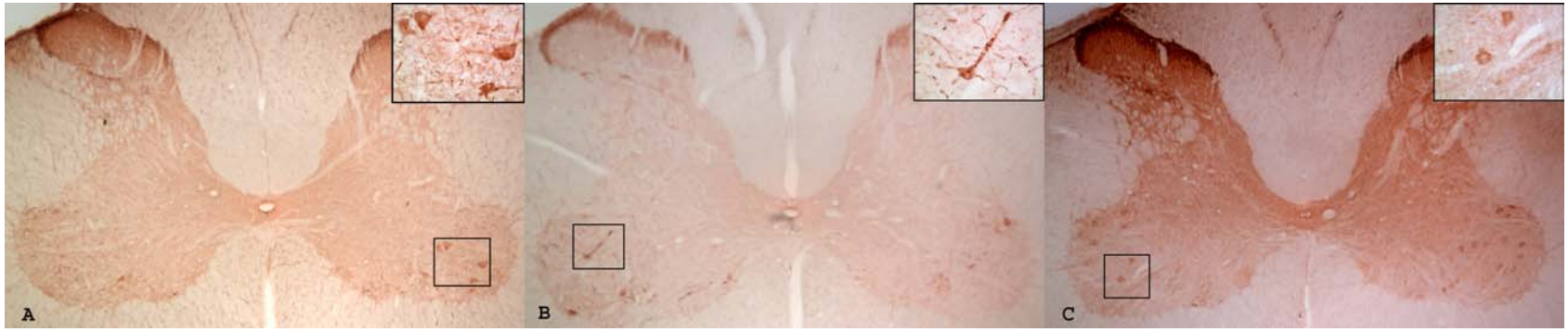

Figure 5-6 CGRP immunolabeling of cervical spinal cord sections. The squares in low magnification pictures denote the locations of the insets. (A) and (B) are from ALS endstage animals treated with rAAV5 GFP and GDNF respectively. (C) Labeling in a wild type littermate. CGRP labels lower motor neurons and the superficial dorsal horns. There was no obvious difference in LMN staining intensity between GDNF and GFP animals.

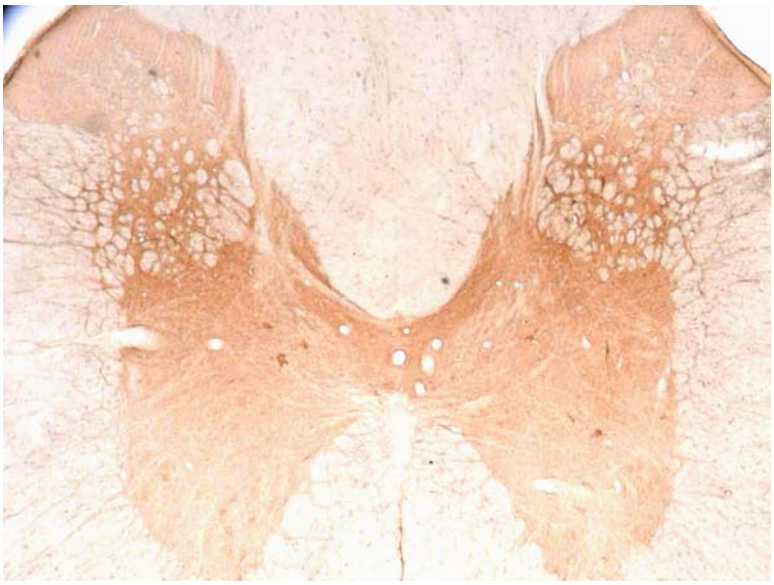

Figure 5-7 GDNF IHC in the spinal cord after bilateral RN injection of rAAV5 GDNF. There is a gradient of staining moving from the dorsal horns to the ventral horns. There are also GDNF+ cell bodies seen in the grey matter.

APPENDIX
PLASMID MAPS

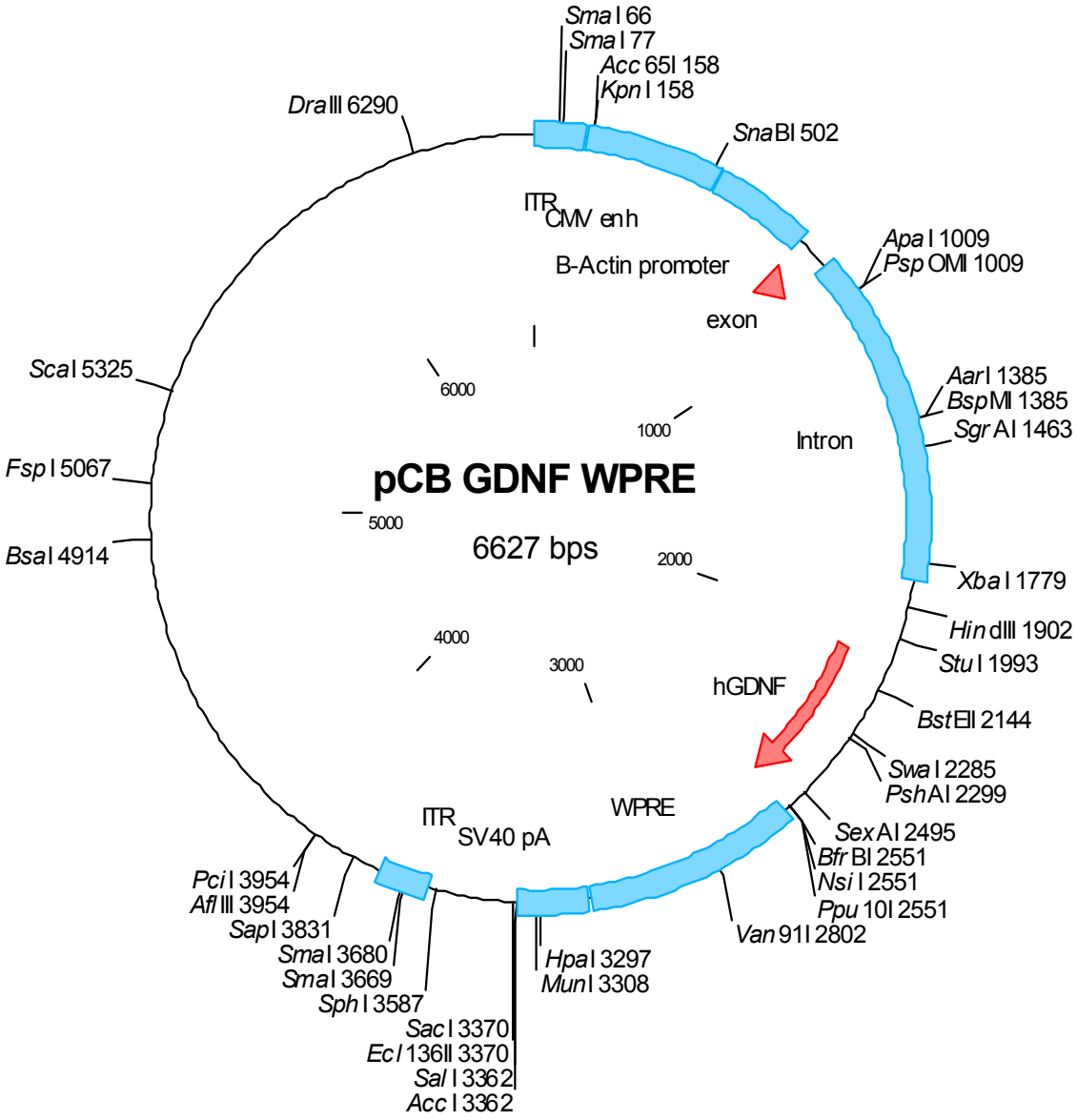

Figure A-1 Plasmid map of pCB GDNF WPRE and UF1. ITR = Inverted Terminal Repeat, TR = Terminal Repeat, CMV enh = cytomegalovirus immediate early enhancer, CB promoter = Chicken β-Actin hybrid promoter, Exon = Chicken β-Actin exon 1, Intron = Chicken β-Actin/Rabbit β-globin hybrid intron, hGDNF = human Glial Cell Derived Neurotrophic Factor cDNA, WPRE = Woodchuck Hepatitis Virus Posttranscriptional Regulatory Element, SV40 pA = simian virus 40 poly adenylation sequence, PYF441 enhancer = enhancer from polyoma virus, HSV-tk = Herpes Simplex Virus Thymidine Kinase promoter, neoR = cDNA encoding for neomycin resistance and ApR = cDNA for ampicillin resistance.

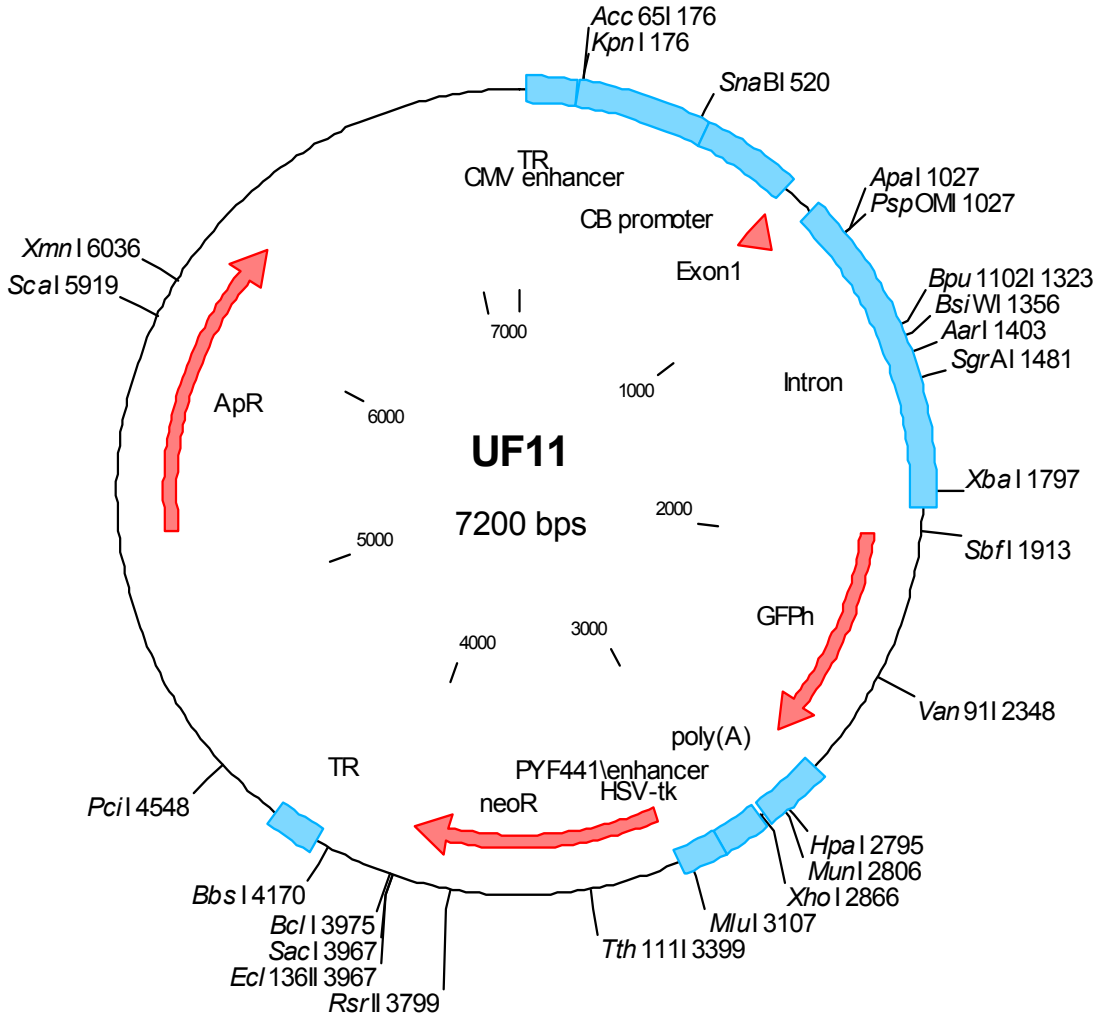

Figure A-1 continued

LIST OF REFERENCES

1. Monani, U. R. (2005) *Neuron* 48, 885-896.

2. Le, T. T., Pham, L. T., Butchbach, M. E., Zhang, H. L., Monani, U. R., Coovert, D. D., Gavrilina, T. O., Xing, L., Bassell, G. J. & Burghes, A. H. (2005) *Hum Mol Genet* 14, 845-857.

3. Lefebvre, S., Burglen, L., Reboullet, S., Clermont, O., Burlet, P., Viollet, L., Benichou, B., Cruaud, C., Millasseau, P., Zeviani, M. & et al. (1995) *Cell* 80, 155-165.

4. Lorson, C. L., Hahnen, E., Androphy, E. J. & Wirth, B. (1999) *Proc Natl Acad Sci U S A* 96, 6307-6311.

5. Monani, U. R., Lorson, C. L., Parsons, D. W., Prior, T. W., Androphy, E. J., Burghes, A. H. & McPherson, J. D. (1999) *Hum Mol Genet* 8, 1177-1183.

6. Cartegni, L. & Krainer, A. R. (2002) *Nat Genet* 30, 377-384.

7. Kashima, T. & Manley, J. L. (2003) *Nat Genet* 34, 460-463.

8. Coovert, D. D., Le, T. T., McAndrew, P. E., Strasswimmer, J., Crawford, T. O., Mendell, J. R., Coulson, S. E., Androphy, E. J., Prior, T. W. & Burghes, A. H. (1997) *Hum Mol Genet* 6, 1205-1214.

9. Lefebvre, S., Burlet, P., Liu, Q., Bertrandy, S., Clermont, O., Munnich, A., Dreyfuss, G. & Melki, J. (1997) *Nat Genet* 16, 265-269.

10. DiDonato, C. J., Chen, X. N., Noya, D., Korenberg, J. R., Nadeau, J. H. & Simard, L. R. (1997) *Genome Res* 7, 339-352.

11. Viollet, L., Bertrandy, S., Bueno Brunialti, A. L., Lefebvre, S., Burlet, P., Clermont, O., Cruaud, C., Guenet, J. L., Munnich, A. & Melki, J. (1997) *Genomics* 40, 185-188.

12. Schrank, B., Gotz, R., Gunnersen, J. M., Ure, J. M., Toyka, K. V., Smith, A. G. & Sendtner, M. (1997) *Proc Natl Acad Sci U S A* 94, 9920-9925.

13. Hsieh-Li, H. M., Chang, J. G., Jong, Y. J., Wu, M. H., Wang, N. M., Tsai, C. H. & Li, H. (2000) *Nat Genet* 24, 66-70.

14. Monani, U. R., Sendtner, M., Coovert, D. D., Parsons, D. W., Andreassi, C., Le, T. T., Jablonka, S., Schrank, B., Rossol, W., Prior, T. W., Morris, G. E. & Burghes, A. H. (2000) *Hum Mol Genet* 9, 333-339.

15. Feldkotter, M., Schwarzer, V., Wirth, R., Wienker, T. F. & Wirth, B. (2002) *Am J Hum Genet* 70, 358-368.

16. McAndrew, P. E., Parsons, D. W., Simard, L. R., Rochette, C., Ray, P. N., Mendell, J. R., Prior, T. W. & Burghes, A. H. (1997) *Am J Hum Genet* 60, 1411-1422.

17. Frugier, T., Tiziano, F. D., Cifuentes-Diaz, C., Miniou, P., Roblot, N., Dierich, A., Le Meur, M. & Melki, J. (2000) *Hum Mol Genet* 9, 849-858.

18. Cifuentes-Diaz, C., Frugier, T., Tiziano, F. D., Lacene, E., Roblot, N., Joshi, V., Moreau, M. H. & Melki, J. (2001) *J Cell Biol* 152, 1107-1114.

19. Vitte, J. M., Davoult, B., Roblot, N., Mayer, M., Joshi, V., Courageot, S., Tronche, F., Vadrot, J., Moreau, M. H., Kemeny, F. & Melki, J. (2004) *Am J Pathol* 165, 1731-1741.

20. Monani, U. R., Pastore, M. T., Gavrilina, T. O., Jablonka, S., Le, T. T., Andreassi, C., DiCocco, J. M., Lorson, C., Androphy, E. J., Sendtner, M., Podell, M. & Burghes, A. H. (2003) *J Cell Biol* 160, 41-52.

21. Liu, Q., Fischer, U., Wang, F. & Dreyfuss, G. (1997) *Cell* 90, 1013-1021.

22. Yong, J., Wan, L. & Dreyfuss, G. (2004) *Trends Cell Biol* 14, 226-232.

23. Carissimi, C., Saieva, L., Gabanella, F. & Pellizzoni, L. (2006) *J Biol Chem* 281, 37009-37016.

24. Ogawa, C., Usui, K., Aoki, M., Ito, F., Itoh, M., Kai, C., Kanamori-Katayama, M., Hayashizaki, Y. & Suzuki, H. (2007) *J Biol Chem*.

25. Winkler, C., Eggert, C., Gradl, D., Meister, G., Giegerich, M., Wedlich, D., Laggerbauer, B. & Fischer, U. (2005) *Genes Dev* 19, 2320-2330.

26. Fan, L. & Simard, L. R. (2002) *Hum Mol Genet* 11, 1605-1614.

27. Zhang, H., Xing, L., Rossoll, W., Wichterle, H., Singer, R. H. & Bassell, G. J. (2006) *J Neurosci* 26, 8622-8632.

28. Zhang, H. L., Pan, F., Hong, D., Shenoy, S. M., Singer, R. H. & Bassell, G. J. (2003) *J Neurosci* 23, 6627-6637.

29. Setola, V., Terao, M., Locatelli, D., Bassanini, S., Garattini, E. & Battaglia, G. (2007) *Proc Natl Acad Sci U S A* 104, 1959-1964.

30. Carrel, T. L., McWhorter, M. L., Workman, E., Zhang, H., Wolstencroft, E. C., Lorson, C., Bassell, G. J., Burghes, A. H. & Beattie, C. E. (2006) *J Neurosci* 26, 11014-11022.

31. Kunst, C. B. (2004) *Am J Hum Genet* 75, 933-947.

32. Reaume, A. G., Elliott, J. L., Hoffman, E. K., Kowall, N. W., Ferrante, R. J., Siwek, D. F., Wilcox, H. M., Flood, D. G., Beal, M. F., Brown, R. H., Jr., Scott, R. W. & Snider, W. D. (1996) *Nat Genet* 13, 43-47.

33. Dal Canto, M. C. & Gurney, M. E. (1995) *Brain Res* 676, 25-40.

34. Gurney, M. E., Pu, H., Chiu, A. Y., Dal Canto, M. C., Polchow, C. Y., Alexander, D. D., Caliendo, J., Hentati, A., Kwon, Y. W., Deng, H. X. & et al. (1994) *Science* 264, 1772-1775.

35. Howland, D. S., Liu, J., She, Y., Goad, B., Maragakis, N. J., Kim, B., Erickson, J., Kulik, J., DeVito, L., Psaltis, G., DeGennaro, L. J., Cleveland, D. W. & Rothstein, J. D. (2002) *Proc Natl Acad Sci U S A* 99, 1604-1609.

36. Nagai, M., Aoki, M., Miyoshi, I., Kato, M., Pasinelli, P., Kasai, N., Brown, R. H., Jr. & Itoyama, Y. (2001) *J Neurosci* 21, 9246-9254.

37. Bruijn, L. I., Miller, T. M. & Cleveland, D. W. (2004) *Annu Rev Neurosci* 27, 723-749.

38. Beckman, J. S. (1994) *Ann N Y Acad Sci* 738, 69-75.

39. Wang, J., Slunt, H., Gonzales, V., Fromholt, D., Coonfield, M., Copeland, N. G., Jenkins, N. A. & Borchelt, D. R. (2003) *Hum Mol Genet* 12, 2753-2764.

40. Woulfe, J. M. (2007) *Neuropathol Appl Neurobiol* 33, 2-42.

41. Shibata, N., Asayama, K., Hirano, A. & Kobayashi, M. (1996) *Dev Neurosci* 18, 492-498.

42. Higgins, C. M., Jung, C. & Xu, Z. (2003) *BMC Neurosci* 4, 16.

43. Guegan, C., Vila, M., Rosoklija, G., Hays, A. P. & Przedborski, S. (2001) *J Neurosci* 21, 6569-6576.

44. Pasinelli, P., Houseweart, M. K., Brown, R. H., Jr. & Cleveland, D. W. (2000) *Proc Natl Acad Sci U S A* 97, 13901-13906.

45. Dupuis, L., Oudart, H., Rene, F., Gonzalez de Aguilar, J. L. & Loeffler, J. P. (2004) *Proc Natl Acad Sci U S A* 101, 11159-11164.

46. Kriz, J., Nguyen, M. D. & Julien, J. P. (2002) *Neurobiol Dis* 10, 268-278.

47. Van Den Bosch, L., Tilkin, P., Lemmens, G. & Robberecht, W. (2002) *Neuroreport* 13, 1067-1070.

48. Gong, Y. H., Parsadanian, A. S., Andreeva, A., Snider, W. D. & Elliott, J. L. (2000) *J Neurosci* 20, 660-665.

49. Lino, M. M., Schneider, C. & Caroni, P. (2002) *J Neurosci* 22, 4825-4832.

50. Pramatarova, A., Laganiere, J., Roussel, J., Brisebois, K. & Rouleau, G. A. (2001) *J Neurosci* 21, 3369-3374.

51. Clement, A. M., Nguyen, M. D., Roberts, E. A., Garcia, M. L., Boillee, S., Rule, M., McMahon, A. P., Doucette, W., Siwek, D., Ferrante, R. J., Brown, R. H., Jr., Julien, J. P., Goldstein, L. S. & Cleveland, D. W. (2003) *Science* 302, 113-117.

52. Wu, Z., Asokan, A. & Samulski, R. J. (2006) *Mol Ther* 14, 316-327.

53. Berns, K. I. (1990) *Microbiol Rev* 54, 316-329.

54. Carter, B. J. (2004) *Mol Ther* 10, 981-989.

55. McCarty, D. M., Young, S. M., Jr. & Samulski, R. J. (2004) *Annu Rev Genet* 38, 819-845.

56. Flotte, T. R., Afione, S. A., Solow, R., Drumm, M. L., Markakis, D., Guggino, W. B., Zeitlin, P. L. & Carter, B. J. (1993) *J Biol Chem* 268, 3781-3790.

57. Haberman, R. P., McCown, T. J. & Samulski, R. J. (2000) *J Virol* 74, 8732-8739.

58. Xie, Q., Bu, W., Bhatia, S., Hare, J., Somasundaram, T., Azzi, A. & Chapman, M. S. (2002) *Proc Natl Acad Sci U S A* 99, 10405-10410.

59. Girod, A., Ried, M., Wobus, C., Lahm, H., Leike, K., Kleinschmidt, J., Deleage, G. & Hallek, M. (1999) *Nat Med* 5, 1052-1056.

60. Wu, P., Xiao, W., Conlon, T., Hughes, J., Agbandje-McKenna, M., Ferkol, T., Flotte, T. & Muzyczka, N. (2000) *J Virol* 74, 8635-8647.

61. Zolotukhin, S. (2005) *Hum Gene Ther* 16, 551-557.

62. Flotte, T. R. (2005) *Curr Gene Ther* 5, 361-366.

63. Afione, S. A., Conrad, C. K., Kearns, W. G., Chunduru, S., Adams, R., Reynolds, T. C., Guggino, W. B., Cutting, G. R., Carter, B. J. & Flotte, T. R. (1996) *J Virol* 70, 3235-3241.

64. Ponnazhagan, S., Erikson, D., Kearns, W. G., Zhou, S. Z., Nahreini, P., Wang, X. S. & Srivastava, A. (1997) *Hum Gene Ther* 8, 275-284.

65. Young, S. M., Jr., Xiao, W. & Samulski, R. J. (2000) *Methods Mol Biol* 133, 111-126.

66. Hallek, M. & Wendtner, C. M. (1996) *Cytokines Mol Ther* 2, 69-79.

67. Li, J., Dressman, D., Tsao, Y. P., Sakamoto, A., Hoffman, E. P. & Xiao, X. (1999) *Gene Ther* 6, 74-82.

68. Wang, B., Li, J. & Xiao, X. (2000) *Proc Natl Acad Sci U S A* 97, 13714-13719.

69. Watchko, J., O'Day, T., Wang, B., Zhou, L., Tang, Y., Li, J. & Xiao, X. (2002) *Hum Gene Ther* 13, 1451-1460.

70. Song, S., Embury, J., Laipis, P. J., Berns, K. I., Crawford, J. M. & Flotte, T. R. (2001) *Gene Ther* 8, 1299-1306.

71. Wang, L., Nichols, T. C., Read, M. S., Bellinger, D. A. & Verma, I. M. (2000) *Mol Ther* 1, 154-158.

72. Sanlioglu, S., Monick, M. M., Luleci, G., Hunninghake, G. W. & Engelhardt, J. F. (2001) *Curr Gene Ther* 1, 137-147.

73. Yan, Z., Zak, R., Luxton, G. W., Ritchie, T. C., Bantel-Schaal, U. & Engelhardt, J. F. (2002) *J Virol* 76, 2043-2053.

74. Qing, K., Mah, C., Hansen, J., Zhou, S., Dwarki, V. & Srivastava, A. (1999) *Nat Med* 5, 71-77.

75. Summerford, C., Bartlett, J. S. & Samulski, R. J. (1999) *Nat Med* 5, 78-82.

76. Flotte, T., Carter, B., Conrad, C., Guggino, W., Reynolds, T., Rosenstein, B., Taylor, G., Walden, S. & Wetzel, R. (1996) *Hum Gene Ther* 7, 1145-1159.

77. Flotte, T. R., Zeitlin, P. L., Reynolds, T. C., Heald, A. E., Pedersen, P., Beck, S., Conrad, C. K., Brass-Ernst, L., Humphries, M., Sullivan, K., Wetzel, R., Taylor, G., Carter, B. J. & Guggino, W. B. (2003) *Hum Gene Ther* 14, 1079-1088.

78. Moss, R. B., Rodman, D., Spencer, L. T., Aitken, M. L., Zeitlin, P. L., Waltz, D., Milla, C., Brody, A. S., Clancy, J. P., Ramsey, B., Hamblett, N. & Heald, A. E. (2004) *Chest* 125, 509-521.

79. Wagner, J. A., Messner, A. H., Moran, M. L., Daifuku, R., Kouyama, K., Desch, J. K., Manley, S., Norbash, A. M., Conrad, C. K., Friborg, S., Reynolds, T., Guggino, W. B., Moss, R. B., Carter, B. J., Wine, J. J., Flotte, T. R. & Gardner, P. (1999) *Laryngoscope* 109, 266-274.

80. Wagner, J. A., Reynolds, T., Moran, M. L., Moss, R. B., Wine, J. J., Flotte, T. R. & Gardner, P. (1998) *Lancet* 351, 1702-1703.

81. Brantly, M. L., Spencer, L. T., Humphries, M., Conlon, T. J., Spencer, C. T., Poirier, A., Garlington, W., Baker, D., Song, S., Berns, K. I., Muzyczka, N., Snyder, R. O., Byrne, B. J. & Flotte, T. R. (2006) *Hum Gene Ther*.

82. McPhee, S. W., Janson, C. G., Li, C., Samulski, R. J., Camp, A. S., Francis, J., Shera, D., Lioutermann, L., Feely, M., Freese, A. & Leone, P. (2006) *J Gene Med* 8, 577-588.

83. Wagner, J. A., Moran, M. L., Messner, A. H., Daifuku, R., Conrad, C. K., Reynolds, T., Guggino, W. B., Moss, R. B., Carter, B. J., Wine, J. J., Flotte, T. R. & Gardner, P. (1998) *Hum Gene Ther* 9, 889-909.

84. Acsadi, G., Anguelov, R. A., Yang, H., Toth, G., Thomas, R., Jani, A., Wang, Y., Ianakova, E., Mohammad, S., Lewis, R. A. & Shy, M. E. (2002) *Hum Gene Ther* 13, 1047-1059.

85. Xu, K., Uchida, K., Nakajima, H., Kobayashi, S. & Baba, H. (2006) *Spine* 31, 1867-1874.

86. Nakajima, H., Uchida, K., Kobayashi, S., Kokubo, Y., Yayama, T., Sato, R. & Baba, H. (2005) *Neurosci Lett* 385, 30-35.

87. Mazarakis, N. D., Azzouz, M., Rohll, J. B., Ellard, F. M., Wilkes, F. J., Olsen, A. L., Carter, E. E., Barber, R. D., Baban, D. F., Kingsman, S. M., Kingsman, A. J., O'Malley, K. & Mitrophanous, K. A. (2001) *Hum Mol Genet* 10, 2109-2121.

88. Azzouz, M., Le, T., Ralph, G. S., Walmsley, L., Monani, U. R., Lee, D. C., Wilkes, F., Mitrophanous, K. A., Kingsman, S. M., Burghes, A. H. & Mazarakis, N. D. (2004) *J Clin Invest* 114, 1726-1731.

89. Ralph, G. S., Radcliffe, P. A., Day, D. M., Carthy, J. M., Leroux, M. A., Lee, D. C., Wong, L. F., Bilsland, L. G., Greensmith, L., Kingsman, S. M., Mitrophanous, K. A., Mazarakis, N. D. & Azzouz, M. (2005) *Nat Med* 11, 429-433.

90. Azzouz, M., Ralph, G. S., Storkebaum, E., Walmsley, L. E., Mitrophanous, K. A., Kingsman, S. M., Carmeliet, P. & Mazarakis, N. D. (2004) *Nature* 429, 413-417.

91. Kaspar, B. K., Llado, J., Sherkat, N., Rothstein, J. D. & Gage, F. H. (2003) *Science* 301, 839-842.

92. Pirozzi, M., Quattrini, A., Andolfi, G., Dina, G., Malaguti, M. C., Auricchio, A. & Rugarli, E. I. (2006) *J Clin Invest* 116, 202-208.

93. Burger, C., Gorbatyuk, O. S., Velardo, M. J., Peden, C. S., Williams, P., Zolotukhin, S., Reier, P. J., Mandel, R. J. & Muzyczka, N. (2004) *Mol Ther* 10, 302-317.

94. Wang, L. J., Lu, Y. Y., Muramatsu, S., Ikeguchi, K., Fujimoto, K., Okada, T., Mizukami, H., Matsushita, T., Hanazono, Y., Kume, A., Nagatsu, T., Ozawa, K. & Nakano, I. (2002) *J Neurosci* 22, 6920-6928.

95. Lu, Y. Y., Wang, L. J., Muramatsu, S., Ikeguchi, K., Fujimoto, K., Okada, T., Mizukami, H., Matsushita, T., Hanazono, Y., Kume, A., Nagatsu, T., Ozawa, K. & Nakano, I. (2003) *Neurosci Res* 45, 33-40.

96. Kaspar, B. K., Erickson, D., Schaffer, D., Hinh, L., Gage, F. H. & Peterson, D. A. (2002) *Mol Ther* 5, 50-56.

97. Miller, T. M., Kaspar, B. K., Kops, G. J., Yamanaka, K., Christian, L. J., Gage, F. H. & Cleveland, D. W. (2005) *Ann Neurol* 57, 773-776.

98. Murakami, T., Nagano, I., Hayashi, T., Manabe, Y., Shoji, M., Setoguchi, Y. & Abe, K. (2001) *Neurosci Lett* 308, 149-152.

99. Zaiss, A. K. & Muruve, D. A. (2005) *Curr Gene Ther* 5, 323-331.

100. Pezet, S., Krzyzanowska, A., Wong, L. F., Grist, J., Mazarakis, N. D., Georgievska, B. & McMahon, S. B. (2006) *Mol Ther* 13, 1101-1109.

101. Guillot, S., Azzouz, M., Deglon, N., Zurn, A. & Aebischer, P. (2004) *Neurobiol Dis* 16, 139-149.

102. Raoul, C., Abbas-Terki, T., Bensadoun, J. C., Guillot, S., Haase, G., Szulc, J., Henderson, C. E. & Aebischer, P. (2005) *Nat Med* 11, 423-428.

103. Xu, Y., Gu, Y., Wu, P., Li, G. W. & Huang, L. Y. (2003) *Hum Gene Ther* 14, 897-906.

104. Nagano, I., Shiote, M., Murakami, T., Kamada, H., Hamakawa, Y., Matsubara, E., Yokoyama, M., Moritaz, K., Shoji, M. & Abe, K. (2005) *Neurol Res* 27, 768-772.

105. Narai, H., Nagano, I., Ilieva, H., Shiote, M., Nagata, T., Hayashi, T., Shoji, M. & Abe, K. (2005) *J Neurosci Res* 82, 452-457.

106. Watson, G., Bastacky, J., Belichenko, P., Buddhikot, M., Jungles, S., Vellard, M., Mobley, W. C. & Kakkis, E. (2006) *Gene Ther* 13, 917-925.

107. Storkebaum, E., Lambrechts, D., Dewerchin, M., Moreno-Murciano, M. P., Appelmans, S., Oh, H., Van Damme, P., Rutten, B., Man, W. Y., De Mol, M., Wyns, S., Manka, D., Vermeulen, K., Van Den Bosch, L., Mertens, N., Schmitz, C., Robberecht, W., Conway, E. M., Collen, D., Moons, L. & Carmeliet, P. (2005) *Nat Neurosci* 8, 85-92.

108. Passini, M. A., Watson, D. J., Vite, C. H., Landsburg, D. J., Feigenbaum, A. L. & Wolfe, J. H. (2003) *J Virol* 77, 7034-7040.

109. Levites, Y., Jansen, K., Smithson, L. A., Dakin, R., Holloway, V. M., Das, P. & Golde, T. E. (2006) *J Neurosci* 26, 11923-11928.

110. Fu, H., Muenzer, J., Samulski, R. J., Breese, G., Sifford, J., Zeng, X. & McCarty, D. M. (2003) *Mol Ther* 8, 911-917.

111. Rapoport, S. I. (2001) *Expert Opin Investig Drugs* 10, 1809-1818.

112. Wang, Z., Zhu, T., Qiao, C., Zhou, L., Wang, B., Zhang, J., Chen, C., Li, J. & Xiao, X. (2005) *Nat Biotechnol* 23, 321-328.

113. Zhu, T., Zhou, L., Mori, S., Wang, Z., McTiernan, C. F., Qiao, C., Chen, C., Wang, D. W., Li, J. & Xiao, X. (2005) *Circulation* 112, 2650-2659.

114. Pacak, C. A., Mah, C. S., Thattaliyath, B. D., Conlon, T. J., Lewis, M. A., Cloutier, D. E., Zolotukhin, I., Tarantal, A. F. & Byrne, B. J. (2006) *Circ Res* 99, e3-9.

115. Rosenberg, W. S., Breakefield, X. O., DeAntonio, C. & Isacson, O. (1992) *Brain Res Mol Brain Res* 16, 311-315.

116. Chung, Y. H., Joo, K. M., Shin, C. M., Lee, Y. J., Shin, D. H., Lee, K. H. & Cha, C. I. (2003) *Brain Res* 994, 253-259.

117. Kaspar, B. K., Frost, L. M., Christian, L., Umapathi, P. & Gage, F. H. (2005) *Ann Neurol* 57, 649-655.

118. Blits, B., Oudega, M., Boer, G. J., Bartlett Bunge, M. & Verhaagen, J. (2003) *Neuroscience* 118, 271-281.

119. Blits, B., Carlstedt, T. P., Ruitenberg, M. J., de Winter, F., Hermens, W. T., Dijkhuizen, P. A., Claasens, J. W., Eggers, R., van der Sluis, R., Tenenbaum, L., Boer, G. J. & Verhaagen, J. (2004) *Exp Neurol* 189, 303-316.

120. Eaton, M. J., Blits, B., Ruitenberg, M. J., Verhaagen, J. & Oudega, M. (2002) *Gene Ther* 9, 1387-1395.

121. Zolotukhin, S., Potter, M., Zolotukhin, I., Sakai, Y., Loiler, S., Fraites, T. J., Jr., Chiodo, V. A., Phillipsberg, T., Muzyczka, N., Hauswirth, W. W., Flotte, T. R., Byrne, B. J. & Snyder, R. O. (2002) *Methods* 28, 158-167.

122. Bennett, M. R., McGrath, P. A., Davey, D. F. & Hutchinson, I. (1983) *J Comp Neurol* 218, 351-363.

123. Lance-Jones, C. (1982) *Brain Res* 256, 473-479.

124. Nurcombe, V., NcGrath, P. A. & Bennett, M. R. (1981) *Neurosci Lett* 27, 249-254.

125. Rootman, D. S., Tatton, W. G. & Hay, M. (1981) *J Comp Neurol* 199, 17-27.

126. Purves D, A. G., Fitzpatrick D, Katz LC, LaMantia AS, Mcnamara JO, Williams SM (2001) *Neuroscience* (Sinauer, Sunderland, MA).

127. von Bartheld, C. S. (2004) *J Neurobiol* 58, 295-314.

128. Georgievska, B., Kirik, D. & Bjorklund, A. (2002) *Exp Neurol* 177, 461-474.

129. Yang, H. W. & Lemon, R. N. (2003) *Exp Brain Res* 149, 458-469.

130. Kuchler, M., Fouad, K., Weinmann, O., Schwab, M. E. & Raineteau, O. (2002) *J Comp Neurol* 448, 349-359.

131. Joosten, E. A. (1997) *Prog Neurobiol* 53, 1-25.

132. Blesch, A. & Tuszynski, M. H. (2001) *J Comp Neurol* 436, 399-410.

133. Kirik, D., Georgievska, B., Burger, C., Winkler, C., Muzyczka, N., Mandel, R. J. & Bjorklund, A. (2002) *Proc Natl Acad Sci U S A* 99, 4708-4713.

134. Kirik, D., Rosenblad, C., Bjorklund, A. & Mandel, R. J. (2000) *J Neurosci* 20, 4686-4700.

135. Enterzari-Taher, M., Eisen, A., Stewart, H. & Nakajima, M. (1997) *Muscle Nerve* 20, 65-71.

136. Kobbert, C., Apps, R., Bechmann, I., Lanciego, J. L., Mey, J. & Thanos, S. (2000) *Prog Neurobiol* 62, 327-351.

137. Grieb, P. (2004) *Folia Neuropathol* 42, 239-248.

138. Bohn, M. C. (2004) *Exp Neurol* 190, 263-275.

139. Manabe, Y., Nagano, I., Gazi, M. S., Murakami, T., Shiote, M., Shoji, M., Kitagawa, H. & Abe, K. (2003) *Neurol Res* 25, 195-200.

140. Manabe, Y., Nagano, I., Gazi, M. S., Murakami, T., Shiote, M., Shoji, M., Kitagawa, H., Setoguchi, Y. & Abe, K. (2002) *Apoptosis* 7, 329-334.

141. Burman, K., Darian-Smith, C. & Darian-Smith, I. (2000) *J Comp Neurol* 423, 179-196.

142. Llado, J., Haenggeli, C., Pardo, A., Wong, V., Benson, L., Coccia, C., Rothstein, J. D., Shefner, J. M. & Maragakis, N. J. (2006) *Neurobiol Dis* 21, 110-118.

143. Ramer, M. S., Bradbury, E. J., Michael, G. J., Lever, I. J. & McMahon, S. B. (2003) *Eur J Neurosci* 18, 2713-2721.

144. Aoi, M., Date, I., Tomita, S. & Ohmoto, T. (2000) *Neurosci Res* 36, 319-325.

145. Hoane, M. R., Gulwadi, A. G., Morrison, S., Hovanesian, G., Lindner, M. D. & Tao, W. (1999) *Exp Neurol* 160, 235-243.

146. Lapchak, P. A., Jiao, S., Collins, F. & Miller, P. J. (1997) *Brain Res* 747, 92-102.

147. Zhang, J. & Huang, E. J. (2006) *J Neurobiol* 66, 882-895.

148. Mitsuma, N., Yamamoto, M., Li, M., Ito, Y., Mitsuma, T., Mutoh, T., Takahashi, M. & Sobue, G. (1999) *Brain Res* 820, 77-85.

149. Yamamoto, M., Mitsuma, N., Inukai, A., Ito, Y., Li, M., Mitsuma, T. & Sobue, G. (1999) *Neurochem Res* 24, 785-790.

150. Li, W., Brakefield, D., Pan, Y., Hunter, D., Myckatyn, T. M. & Parsadanian, A. (2007) *Exp Neurol* 203, 457-471.

151. Miller, T. M., Kim, S. H., Yamanaka, K., Hester, M., Umapathi, P., Arnson, H., Rizo, L., Mendell, J. R., Gage, F. H., Cleveland, D. W. & Kaspar, B. K. (2006) *Proc Natl Acad Sci U S A* 103, 19546-19551.

152. Traynor, B. J., Bruijn, L., Conwit, R., Beal, F., O'Neill, G., Fagan, S. C. & Cudkowicz, M. E. (2006) *Neurology* 67, 20-27.

153. Mouton, L. J., Klop, E. M. & Holstege, G. (2005) *Brain Res* 1043, 87-94.

154. McGeer, P. L. & McGeer, E. G. (2002) *Muscle Nerve* 26, 459-470.

155. Chang, Y. P., Fang, K. M., Lee, T. I. & Tzeng, S. F. (2006) *J Cell Biochem* 97, 501-511.

BIOGRAPHICAL SKETCH

Kevin David Foust was born in Cleveland, Ohio, on September 12, 1978 to Robert and Janice Foust. His family moved to Orlando, Florida, when he was three. He grew up in the Orlando area before moving to Gainesville, Florida to attend the University of Florida. He was continuously enrolled at UF from August 1997 to May 2007, pursuing both his bachelor's and doctorate degrees. While there he met his wife Abby and celebrated many a Gator athletic triumph.